

5-2016

Thermal conductivity measurements of nanomaterials

Javier Acosta Martinez
The University of Texas Rio Grande Valley

Follow this and additional works at: <https://scholarworks.utrgv.edu/etd>



Part of the [Mechanical Engineering Commons](#)

Recommended Citation

Acosta Martinez, Javier, "Thermal conductivity measurements of nanomaterials" (2016). *Theses and Dissertations*. 105.

<https://scholarworks.utrgv.edu/etd/105>

This Thesis is brought to you for free and open access by ScholarWorks @ UTRGV. It has been accepted for inclusion in Theses and Dissertations by an authorized administrator of ScholarWorks @ UTRGV. For more information, please contact justin.white@utrgv.edu, william.flores01@utrgv.edu.

THERMAL CONDUCTIVITY MEASUREMENTS
OF NANOMATERIALS

A Thesis

by

JAVIER ACOSTA MARTINEZ

Submitted to the Graduate College of
The University of Texas Rio Grande Valley
In partial fulfillment of the requirements for the degree of

MASTER OF SCIENCE

May 2016

Major Subject: Mechanical Engineering

THERMAL CONDUCTIVITY MEASUREMENTS
OF NANOMATERIALS

A Thesis
by
JAVIER ACOSTA MARTINEZ

COMMITTEE MEMBERS

Dr. Karen Lozano
Co-chair of Committee

Dr. Young-Gil Park
Co-chair of Committee

Dr. Mataz Alcoutlabi
Committee Member

May 2016

Copyright 2016 Javier Acosta Martinez

All Rights Reserved

ABSTRACT

Acosta Martinez, Javier, Thermal Conductivity Measurements of Nanomaterials. Master of Science (MS), May, 2016, 81 pp., 10 tables, 33 figures, references, 82 titles.

Thermal conductivity “k” can be defined as a material property where heat is diffused due to a temperature gradient within the material. A study was made to compare the different types of studies of thermal conductivity of nanomaterials, as well as, a comparison among the different types of setups used to measure thermal conductivity. For this study a custom made thermal conductivity tester was built, this tester was validated by measuring materials with both low and high thermal conductivity, and comparing the results with the ones found in literature. After the validation, materials with unknown thermal conductivity were measured. The low thermal conductivity material was PVDF along with PVDF samples that contained different wt% of boron nitride. The high thermal conductive material was carbonized PVA fibers, the carbonized PVA fibers showed an increment of almost 10 times what was recorded for the pre-carbonized PVA sample.

DEDICATION

The completion of my graduate studies would not have been possible without the unconditional love, and support from my family. My father Santos Acosta Palacios, my mother, Virginia Martinez Gutierrez, my brothers, Santos Acosta Martinez, and Jesus Acosta Martinez. I would also like to dedicate this to my friends for their support through my undergraduate and graduate studies

ACKNOWLEDGMENTS

I will always be grateful to Dr. Karen Lozano, co-chair of my dissertation committee, for giving me the opportunity to start working with her, as an undergraduate research assistant. Without her advice and mentoring none of this would be possible. Thank you for believing in me, and for reminding me that in order to become better person, you have to strive for success, and also to never ever stop learning. It has been a privilege to work with you. To Dr. Young-Gil Park, co-chair, thank you for your aid, advice and input, also without you none of this would be possible. To Dr. Mataz Alcoutlabi, my dissertation committee member: your comments, and suggestions on my dissertation work helped to improve, and have a great quality of work at the end.

I would also like to thank Dr. Lee Cremer and the rest of my colleagues from the PREM research group for their support through this time.

TABLE OF CONTENTS

	Page
ABSTRACT.....	iii
DEDICATION.....	iv
ACKNOWLEDGEMENTS.....	v
TABLE OF CONTENTS.....	vi
LIST OF TABLES.....	viii
LIST OF FIGURES.....	ix
CHAPTER I. INTRODUCTION.....	1
1.1 Background.....	1
1.2 Literature Review.....	3
1.2.1 Thermal Conductivity of Nanofibers and Their Composites.....	3
1.2.2 Carbon Fibers.....	3
1.2.3 Composites.....	12
1.2.4 Mats.....	27
1.2.5 Thin Films.....	31
1.2.6 Carbon Nanotubes.....	33
1.3 Methods to Measure Thermal Conductivity.....	35
1.3.1 Guarded Hot Plate Method.....	35
1.3.2 Laser Flash Method.....	38

1.3.3 Microfabricated Device.....	39
1.3.4 Kohlrausch Method.....	42
1.3.5 Hot-wire Method.....	43
1.3.6 Non-contact Optical Based Technique.....	45
1.3.7 Dual Mode Heat Flow Meter.....	46
CHAPTER II. EXPERIMENTAL SETUP.....	50
CHAPTER III. RESULTS AND DISCUSSION.....	55
CHAPTER IV. CONCLUSION AND FUTURE WORK.....	69
REFERENCES.....	71
APPENDIX.....	79
BIOGRAPHICAL SKETCH.....	81

LIST OF TABLES

	Page
Table 1: VGCF/phenolic composite thermal conductivities.....	13
Table 2: Comparison between the different thermal conductivity setups	48
Table 3: In-plane thermal conductivity of known materials by using the thermal conductivity setup.....	59
Table 4: PVDF samples thermal conductivity measurements.....	60
Table 5: PVA samples thermal conductivity.....	61
Table 6: Thermal conductivity of the PVA carbonized samples.....	62
Table 7: Thermal conductivity of the copper foil samples.....	63
Table 8: Thickness and thermal conductivity comparison of the sample material.....	65
Table 9: Area density analysis of the sample material.....	66
Table 10: Thermal Conductivity of the samples measured using the thermal conductivity setup	67

LIST OF FIGURES

	Page
Figure 1: a) In-plane direction and b) through-plane direction	2
Figure 2: Axial direction and lateral direction	3
Figure 3: Bundle of ribbon fibers prepared for thermal conductivity measurement using Angstrom's apparatus.....	4
Figure 4: Schematic of the Angstrom's Apparatus	4
Figure 5: Schematic of the thermal potentiometer	5
Figure 6: a) Thermal conductivity measurements using the Armstrong apparatus, and b) Thermal conductivity measurements using the thermal potentiometer.....	5
Figure 7: Schematic diagram of the experimental apparatus and measurement system: 1-vacuum pump; 2-molecular pump; 3-heat sink; 4-hot wire; 5-tested fiber; 6-multimeter; 7-resistance; 8- power supply; 9-temperature controller; 10-exhausted valve; 11-liquid N2 inlet & outlet; 12- pressure gauge	6
Figure 8: Schematic explaining the linear dependence of the thermal resistivity on the specimen thickness.....	10
Figure 9: Schematic of the thermal comparative method.....	15
Figure 10: Schematic of the thermal conductivity setup.....	22
Figure 11: Schematic of the thermal conductivity setup	23

Figure 12: Schematic diagram of the experimental setup	24
Figure 13: Schematic of the thermal conductivity setup.....	28
Figure 14: Thermal conductivity of mats as a function of the volume fraction of nanofibers.....	29
Figure 15: Guarded Hot Plate method set up for measuring thermal conductivity.....	36
Figure 16: Schematic explaining the linear dependence of the thermal resistivity on the specimen thickness	38
Figure 17: Microfabricated device	40
Figure 18: Experimental setup for the Kohlrausch method.....	42
Figure 19: Hot wire setup.....	44
Figure 20: Non-contact optical based technique schematic	46
Figure 21: Dual mode heat flow meter	46
Figure 22: SolidWorks model of the copper material and the unknown material, for this instance carbon fiber.....	51
Figure 23: SolidWorks model of the thermal conductivity test setup.....	51
Figure 24: Aluminum plate where the setup was mounted	52
Figure 25: Acrylic bell jar (12"x12"x0.5").....	52
Figure 26: Thermocouple inside the feedthrough and compression fitting.....	53
Figure 27: Copper foil being measured by the thermal conductivity tester.....	54
Figure 28: Carbon nanofibers being measured by the thermal conductivity tester.....	54
Figure 29: Thermostatic water bath used for thermocouple calibration.....	55
Figure 30: PVDF Sample	60
Figure 31: Carbonized PVA sample	62
Figure 32: Copper foil	63

Figure 33: Comparing the relationship between the sample thickness and its thermal conductivity 64

CHAPTER I

INTRODUCTION

1.1 Background

Thermal conductivity “k” can be defined as a material property where heat is diffused due to a temperature gradient within the material—the property of a material to conduct heat. Materials with a high thermal conductivity are called conductors, the ones with a low thermal conductivity are called insulators.

For thin materials, there are a variety of methods to measure “k” depending on direction of heat transfer: in-plane or through plane. The in-plane thermal conductivity of a material can be measured on two different directions, parallel also known as axial, and perpendicular or lateral. Depending on the isometry of the material, there is a significant difference in the values obtained from the thermal conductivity measurements in the axial and lateral directions. The chosen method is based on the foreseen application, if heat is needed to be dissipated within the surface or through the sample.

Thermal conductivity can be applied on a variety of sectors, such as: thermoelectrics, thermal interface materials, thin films, insulation, cement and concrete, heat transfer fluids, nanomaterials, among many others. When evaluating the measurements of thermal conductivity

from nanomaterials (nanofibers), there are a variety of methods to obtain the thermal conductivity. However, a lot of these methods, measure the thermal conductivity in an indirect form. This means that the thermal conductivity is obtained based on external factors, such as: thermal diffusivity, specific heat, electrical resistivity, thermal resistivity, etc. On the other hand, while there are methods that measure the thermal conductivity with a simple formula and in a direct way, a lot of methods obtain the thermal conductivity with complex equations.

A study was done to evaluate different cases of nanomaterials, such as: carbon fibers, composites, mats, thin films, carbon nanotubes, as well as, different thermal conductivity setups were studied, and compared. The objective being, to construct an apparatus that could measure the thermal conductivity of nanomaterials (nanofibers).

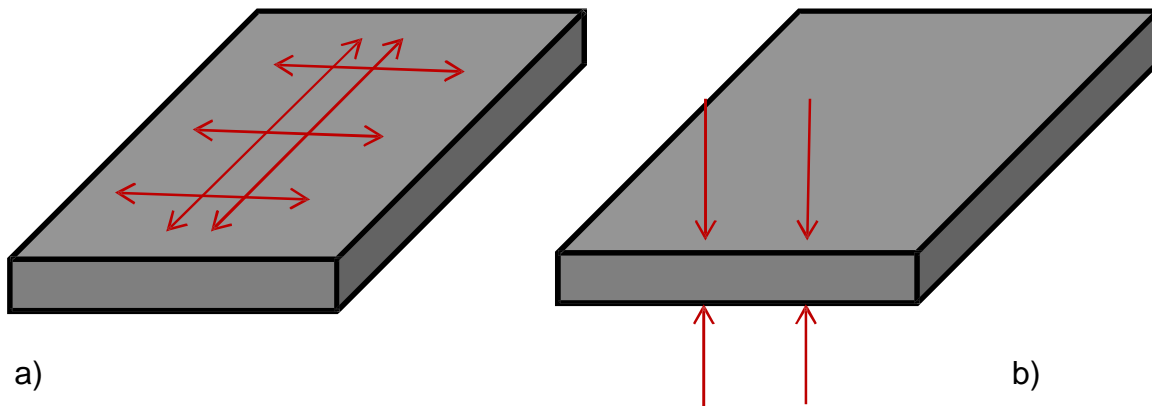


Figure 1. a) In-plane direction and b) through-plane direction

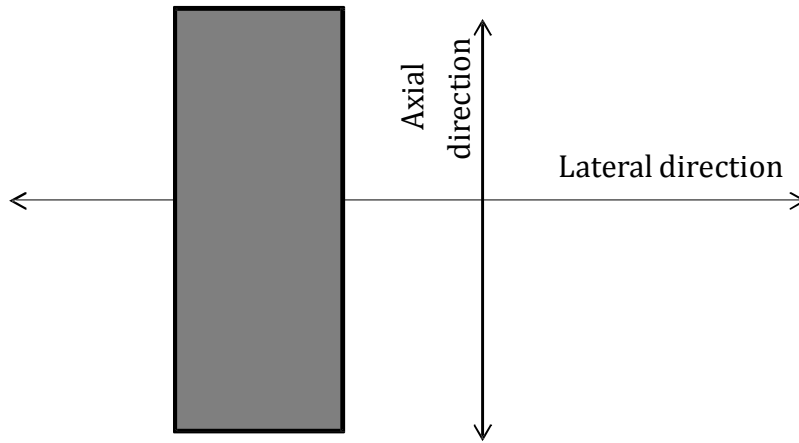


Figure 2. Axial direction and lateral direction

1.2 Literature Review

1.2.1 Thermal Conductivity of Nanofibers and their Composites

The following sections will present a review of previous studies on thermal conductivity measurements of nanofiber and composite materials. The review includes types of materials, brief descriptions of their preparation methods, as well as the thermal conductivity test methods used for evaluating the materials.

1.2.2 Carbon Fibers

Gallego et. Al [1] performed testing with different ribbon-shaped fibers, one group of fibers was made at Clemson University, where these fibers were graphitized at a temperature of 2400 °C, and the other group consisted of commercial carbon fibers, which were graphitized at 3000 °C. There were 2 different types of measurements for these fibers. The Angstrom's apparatus, (Figure 4.) which measured the thermal conductivity against the electrical resistivity of the fibers at room temperature, and the thermal potentiometer (Figure 5.), which measures the

thermal response of a fiber sample at a fixed temperature. The data obtained in both figures shows that the temperature dependence of thermal conductivity and electrical resistivity is similar to commercial fibers.

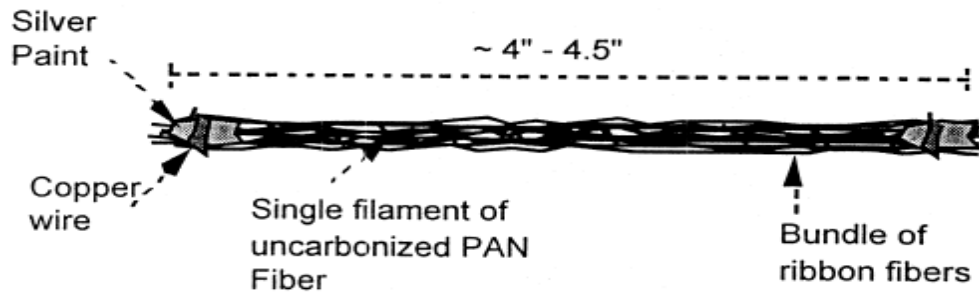


Figure 3. Bundle of ribbon fibers prepared for thermal conductivity measurement using Angstrom's apparatus [1].

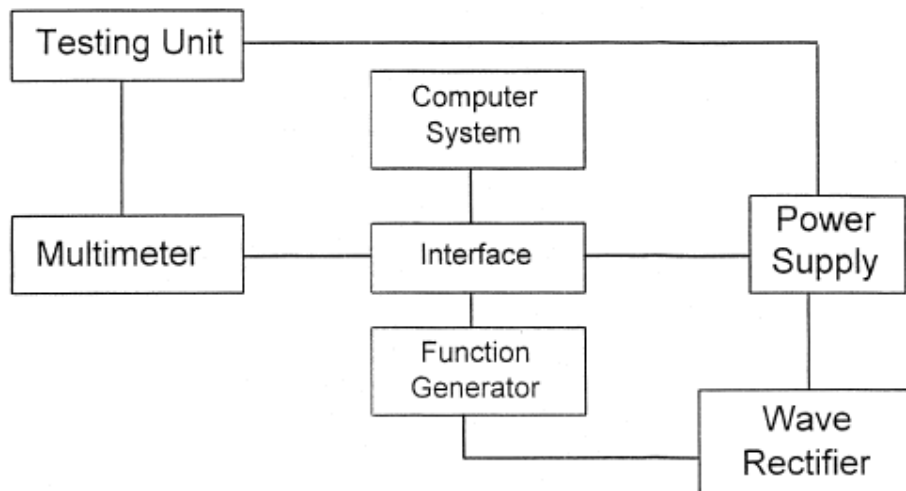


Figure 4. Schematic of the Angstrom's Apparatus [1].

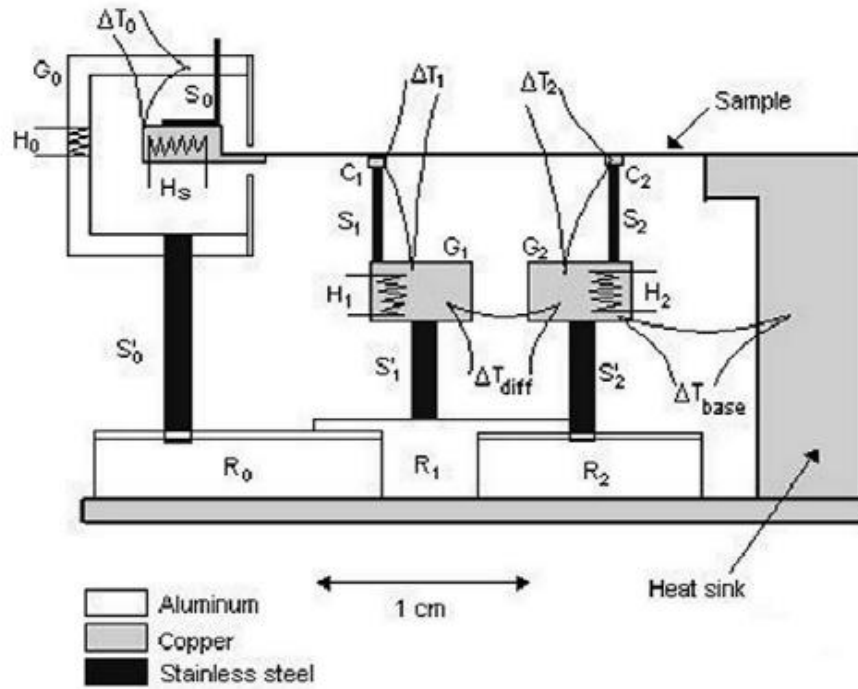


Figure 5. Schematic of the thermal potentiometer [1].

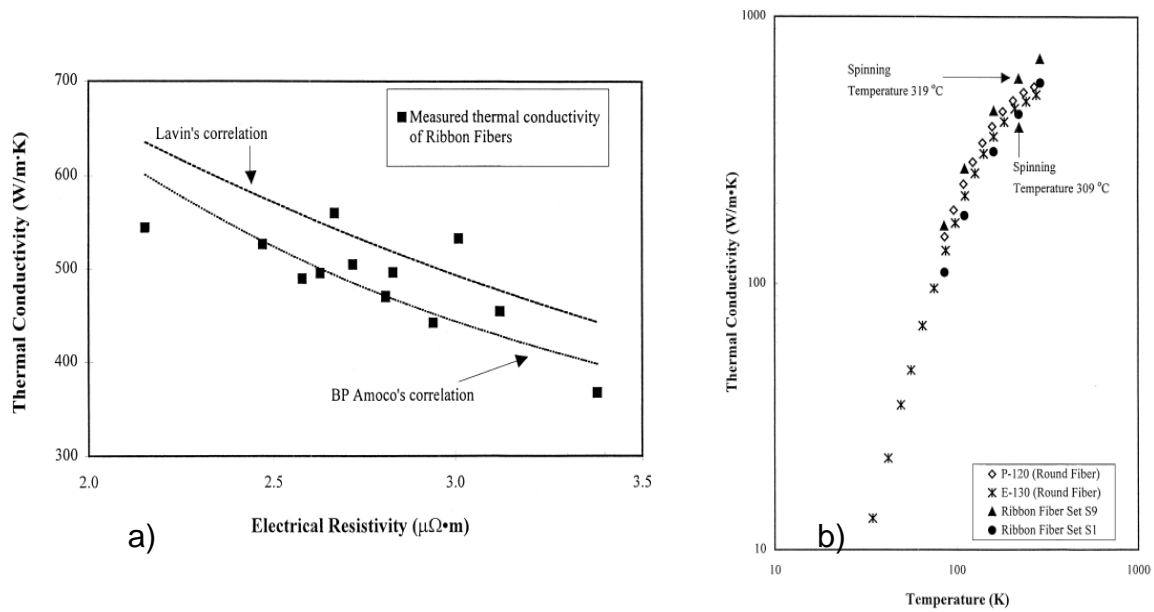


Figure 6. a) Thermal conductivity measurements using the Armstrong apparatus, and b) Thermal conductivity measurements using the thermal potentiometer [1].

Wang et al. [2] performed measurements of single-pitch carbon fibers ranging between 100 °C – 400 °C, via a T type method, where a wire served as a heating source as well as a thermometer, with this T type method, the thermal properties of the hot wire were measured. During the testing, a carbon fiber was attached to the center position of the wire, where thermal conductivity was measured by doing a comparison between the change of temperature of the hot wire, with and without the carbon fiber.

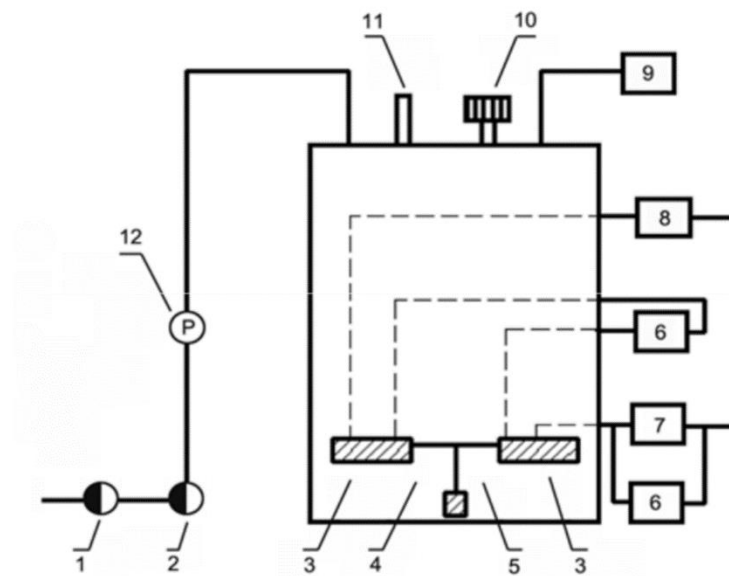


Figure 7. Schematic diagram of the experimental apparatus and measurement system: 1-vacuum pump; 2-molecular pump; 3-heat sink; 4-hot wire; 5-tested fiber; 6-multimeter; 7-resistance; 8-power supply; 9-temperature controller; 10-exhausted valve; 11-liquid N2 inlet & outlet; 12-pressure gauge [2].

Hyun et al. [3] used two types of carbon fiber reinforcements for the fabrication of Carbon–Carbon composites. [Semi-random chopped PAN based carbon fibers with one layer of fabric were used as a reinforcement in the friction surface and 8 H/S PAN based carbon fabrics

were used as load-bearing components of C–C composites. By using different fibers and techniques 7 different types of fibers were prepared: Type I specimen was laid up and cured in a hot press with chopped PAN-based fiber graphitized at 2000 °C. Type II-a preform was fabricated with chopped fibers graphitized at 2400 °C . Type II-b specimen, reinforced with chopped fiber graphitized at 2400 °C. Type III-a specimen, reinforced with chopped fiber graphitized at 2800 °C. Type III-b specimen, reinforced with chopped fibers graphitized at 2800 °C. Type IV and Type V specimens, reinforced with chopped fibers graphitized at 2400 °C. The thermal conductivity of the carbon-carbon composite is affected by factors such as the kind of fiber and matrix carbon, the method of heat treatment, bulk density, temperature applied on the sample, etc. Thermal conductivity for parallel and normal direction to the plane of frictional surface was measured at room temperature with a dynamometer test machine. The friction coefficient and wear rates were found to decrease as thermal conductivity increases.

Moses Jr [4] investigated the case where it was necessary to determine the thermal conductivity of carbon fibers, in order to use them on re-entry nose cones, for the US Air Force. But the desire in this experiment was not to get a high thermal conductivity from the PAN fibers, but rather obtain low thermal conductivity from them. Two different types of samples: a pure fiber specimen and a composite specimen. The pure fiber specimen was fabricated void of air, since it was considered that an air fiber composite system would decrease the thermal conductivity of the fibers. The observation was noted by that carbon fibers are anisotropic, with the transverse thermal conductivity of the fiber being much lower than the axial conductivity. Consequently, the fiber bundle must be kept in relatively perfect alignment in order to prevent the introduction of a large thermal resistance at each end of the specimen. As for the composite specimen, it was made from an epoxy resin based material that was developed in order to

maintain the fiber alignment and also remove air voids. In order to measure thermal conductivity, a guarded hot plate apparatus was used to get these measurements, this method was chosen because it was accurate and simple according to the author. The fibers measured that had the epoxy resin had a very low thermal conductivity this being around 3.4-4.6 W/m*K it can be assumed that the results are lower than the regular fiber because the epoxy is acting as an insulator, preventing the proper thermal conductivity on the sample.

Gallego et al. [5] determined that in order to melt-spin mesophase pitch fiber successfully the temperature range is very important, because decreasing the temperature even if it is only for a few degrees, this increases the viscosity and it can induce a brittle fracture during the drawdown. Whereas increasing the temperature while it reduces the viscosity, it can cause a thermal degradation. They also mention that the spinning temperature not only affects the uniformity of the fiber, but it also influences their molecular orientation. These fibers were produced at a spinning temperature that varied from 305 °C to 325 °C with increments of 5 °C. After these fibers were obtained they were oxidized in air at 280 °C for 30 min, and finally they were graphitized in an inert atmosphere at 2400 °C. The fibers were subjected to thermal conductivity testing, using two different methods the authors have previously used, the Angstrom's apparatus and the thermal potentiometer. Results show that the thermal conductivity and degree of graphitization increase as spinning temperature increases until both reach a maximum. Then, any additional increase in spinning temperature causes a decrease in thermal conductivity and degree of graphitization. However, the degree of graphitization decreases more dramatically than the thermal conductivity.

Chen et al. [6] prepared three different kinds of PAN based carbon fibers (T700, T300, M40), these fibers endured heat treatment at 3 different temperatures, 2000 C, 2300 C, and finally 2500 C. It was determined that the carbon fibers, and carbon matrix are the main channels for heat conduction of carbon composite. Where the carbon fibers are the primary heat transfer channel for thermal conductivity along the fiber axis, and the carbon matrix is the primary heat transfer channel for thermal conductivity in the perpendicular direction of the fiber axis. The thermal conductivity of the samples was measured by using an X-ray diffraction analyzer as well as a polarized light microscope. After obtaining the data, the thermal conductivity was measured with the following formula, $\lambda = 418.68 a C_p d$, where a is the thermal diffusivity, C_p is the specific heat, and d is the density of the composite. The results show that even though the fiber content is the same, after going through the heat treatment at 2500C the graphitization went much higher for the M40 PAN based carbon fibers, as well as the thermal conductivity. It should be also noted that the difference between the thermal conductivity in the parallel direction is at least 10 times higher than the one in the perpendicular direction.

Seungjin et al. [7] improved the through-thickness thermal conductivity of continuous carbon, via a nanostructuring method, this method applied carbon black to the interlaminar interface. The interlaminar interface thickness was successfully increased by applying carbon black, since the thickness of the sample was increased so did the thermal resistivity which can be explained on the Figure 8. The more thickness a sample has the better conductivity it will have, this is due to the method being used for the measurements, which is the guarded hot plate, here they obtain the thermal resistivity and due to the inverse of the slope of the resistivity the thermal conductivity is obtained.

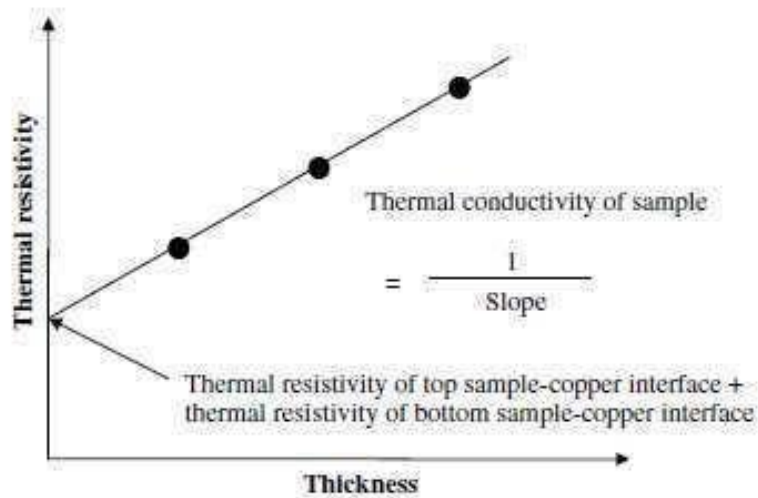


Figure 8. Schematic explaining the linear dependence of the thermal resistivity on the specimen thickness [7].

Korab et al. [8] coated continuous commercial carbon fibers with copper, they performed the thermal conductivity measurements via laser-flash method. The thermal conductivity of the samples was evaluated with increasing carbon content, ranging from 0 to 100%. The results showed that fiber containing a fiber volume fraction of 40% showed the highest measurements of thermal conductivity, rendering results around 230 W/ m*K, while increasing the percentage of fibers present, made the thermal conductivity to go down.

Fukai et al. [9] used carbon fibers intending to enhance the thermal conductivity of energy storage media. Two different enhancement methods were used; one used randomly oriented fibers, while the other one used a fiber brush. The thermal conductivity method used was the laser-flash method, adding randomly oriented fibers did not increase the thermal conductivity considerably, while using the fiber brush increased the thermal conductivity considerably. However the author concluded that even though using the fiber brush was more

useful, the choice of which method to use depends on the structure and type of energy storage media would be used.

Ordonez and Yang [10] coated carbon nanofibers with metallic layer, and they embedded them into a dielectric matrix, what they found out was that the metallic layers enhanced the thermal conductivity of the fibers, when comparing them with the uncoated fibers, they had increment of about 30%, they determined that the thermal conductivity increased along the radius of the fibers, as well as the thickness of the coating and the volume fraction of fibers present.

Zhang et al. [11] used the short hot wire technique in order to evaluate the thermal conductivity of different commercial single fiber carbon samples, the results were similar among the fibers measured, also as the temperature rises so would the thermal conductivity, the authors concluded that by using the average temperature rise as well as the heat generation rate of the hot wire, the thermal conductivity can be easily measured.

May et al. [12] created diamond fibers via chemical vapor deposition, these diamond fibers had tungsten wire with different diameters as the core. The thermal conductivity of the diamond fibers was measured with an apparatus that was made by the authors in order to minimize the heat transfer with the exception the ones along the fiber. The single diamond fibers show values three times the value of copper, and when it is attached to a fiber epoxy composite, the values show great values, as high as 940 W/m-K.

Wolter et al. [13] compared the thermal conductivity of epitaxially textured diamond films, was compared against randomly textured diamond films. The diamond films were grown onto silicon wafer, using chemical vapor deposition. For the thermal conductivity measurements

Joule heating thermometry which measured the temperature gradient along the films in steady-state as a function of the applied power to a heater element, was used. When comparing the results the epitaxially textured diamond films had a greater thermal conductivity, 1120 W/m *K, and the randomly textured diamond films had 550 W/m *K. This shows that controlling the alignment of the fibers improves thermal conductivity drastically.

Ma et al. [14] measured ribbon-shaped mesophase pitch-based carbon fibers were measured via laser-flash method, it was found that the fiber thermal conductivity was affected depending on its fiber orientation. Aligned fibers would have a better thermal conductivity, than compared to the un-oriented fibers.

Mayhew and Prakash [15] evaluated the thermal conductivity of commercially vapor grown carbon fibers, as well as heat-treated and on-heat treated individual carbon nanofibers. The thermal conductivity measurements were performed via T-type probe method. The thermal conductivity measurements showed the heat treated individual carbon nanofibers were the ones that had the best thermal conductivity.

1.2.3 Composites

Patton et al. [16] prepared vapor grown carbon fibers/phenolic resin composites were prepared by high shear mixing followed by thermal curing. 19 different samples were prepared, and used for different types of testing. Samples 3, 7, 11, 15, and 18, shown in Figure () were used for the thermal conductivity testing. The thermal conductivity was measured according to the ASTM C 177-85 standard test method for steady-state heat flux measurements and thermal transition properties using a guarded-hot-plate apparatus. The testing temperature ranged from 22.2 °C to 93.3 °C. Measurements were recorded every 10 minutes for 90 minutes. All of the

samples showed similar thermal conductivities, ranging from .54 to .62 W/m-K, the thermal conductivity of carbon fibers is usually higher than what was measured above, but what affects the thermal conductivity in this case are both the resin covering the VGCF, since it acts as an insulator and that the fiber length is too small, making the samples not heat conductive.

Table 1. VGCF/phenolic composite thermal conductivities [16].

Composite sample number	Fiber wt%	Thermal conductivity (W/m*K)
18	0	0.28 ±0.07
3	30	0.57±0.02
7	40	0.54±0.01
11	40 ^a	0.62±.0.01
15	45/5 ^S	0.57±0.03

a. Ball milled fiber and extra high shear mixing

b. Compacted fiber

Ai-jie et al. [17] tested silicon carbide/ carbon fiber/ epoxy resin composites, thermal conductivity of the samples was measured with a Hot Disk thermal analyzer, the results show that the CF/Epoxy composites increase their thermal conductivity as the volume fraction of SiC added to the composites is increased.

Hyun et al. [18] evaluated the thermal conductivity of polymer composites based on the length of multi-walled carbon nanotubes (MWCNT) was evaluated. Samples were prepared with short and long MWCNTs filled composites with different MWCNT weight fractions. This was done in order to check how the length of the nanotubes would affect the in-plane thermal conductivity of the samples. Results showed that increasing the content of MWCNT reduces the

matrix region between MWCNTs in a composite and facilitates the interaction between MWCNTs, which in turn contributes to the enhancement of thermal conductivity. They said that with these results, they can conclude, when fabricating thermally conductive composite samples with MWCNTs, it is more favorable to enhance in-plane thermal conductivity because MWCNTs are easily oriented in the in-plane direction. A Hot Disk thermal analyzer was used to measure the thermal conductivity.

Ng et al. [19] prepared hybrid composites were prepared, the composites consisted of boron nitride (BN) platelets and carbon fibers (CF) in a polybutylene terephthalate (PBT) matrix. The thermal conductivity of these samples was measured by guarded hot plate method. When evaluating the thermal conductivity, the k value increased as the filler % of BN and CF increased. When comparing the two different composites, the CF had a slightly higher thermal conductivity until 25% wt, after that the thermal conductivity of the BN composite was slightly higher. The measurements of thermal conductivity started at 0.25 W/m*K, when it was the pure PBT matrix, and it peaked at 0.65 and 0.6 W/m*K for the BN and CF composites respectively.

Valipour et al. [20] evaluated The diameter dependence of PMMA nanofibers, the thermal conductivity measurements were performed by the hot-wire method. The results showed that the thinner the PMMA nanofibers were the lower the thermal conductivity would be, even if the results were low with thinner nanofibers, the thermal conductivity still increased as the temperature increased.

Khan et al. [21] prepared PAN and PMMA nanofibers, via electrospinning, which were embedded with graphene nanoflakes, to see if their properties would be enhanced by the addition of the different weight percentages of nanoflakes, thermal conductivities were

determined by the thermal comparative method (Figure 9), as the weight percentage of the nanoflakes increased so did the thermal conductivity, going from 1 to 5 W/m-K, and 1 to 2.5 W/m-K, for the PMMA and PAN fibers respectively, the authors concluded that due to the excellent properties these fibers had, they could be used for batteries and supercapacitors.

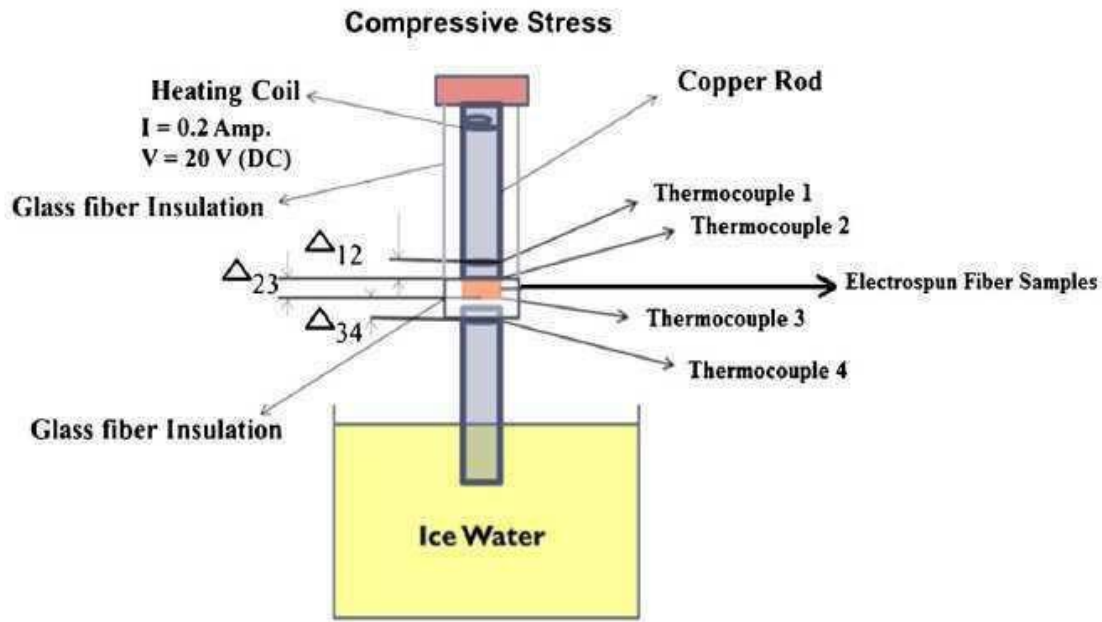


Figure 9. Schematic of the thermal comparative method [21].

Kausar and Ashraf [22] fabricated non-woven, nanofibrous membranes from nano-diamond particles (ND) were fabricated, as well as multi-walled carbon nanotube-filled poly(azo-pyridine) which were prepared by electrospinning. These membranes were added to an epoxy matrix, two different samples were prepared the epoxy composites with MWCNT-PA, and epoxy composites with MWCNT-PA and ND. The MWCNT-PA composites displayed a good values of thermal conductivity, the addition of the ND enhanced the thermal conductivity even more, the measurements were performed via laser flash method.

Liang et al. [23] fabricated carbon fiber composites were fabricated using a vacuum assisted resin transfer molding incorporating the carbon nanofibers. Two different methods were used, matrix modifications and fiber modification routes. The matrix modification procedure consisted on the vapor grown carbon fibers to be added directly into the epoxy resin. The fiber modification route, consisted on the carbon nanofibers were directly grown on the carbon fiber fabric via chemical vapor deposition. The matrix modification route did not show any promising improvements, but on the other hand, the fiber modification route showed great improvement in both in-plane and through thickness thermal conductivity, perhaps this shows it is better to directly grow carbon fiber than rather just add them. The thermal conductivity of the samples was measured via a hotwire 3ω method, the measurements were done at different temperatures.

Weidenfeller et al. [24] evaluated the thermal conductivity of polypropylene (PP) with various fillers (such as Fe_2O_4 , BaSO_4 , Cu, glass fiber, among others) was measured, the filler fraction ranged between 0 to 50% in volume. The thermal conductivity of the PP filled with glass fibre and barite did not show big enhancement on thermal conductivity, while the PP samples filled with copper and talc showed the highest thermal conductivity, having values of 2.2 and 2.6 W/m-K respectively.

Kuriger and Alam [25] prepared composites of polypropylene reinforced with Pyrograf III, laser-flash method was used to measure the thermal conductivity of the samples. The in- plane measurements showed great improvements, when comparing the composite with aligned Pyrograf III fibers, with one that had unaligned fibers. For the transverse direction thermal conductivity there was a considerable enhancement too, both aligned and unaligned fiber composites increased as the fiber % increased, but the aligned fiber composites showed a greater increment in thermal conductivity.

Kim and Kim [26] prepared an ethylene-propylene-diene (EPDM) matrix was prepared, which was added different thermal conductive fillers, synthetic graphite, carbon fiber, and carbon nanotubes. The experimentation consisted in evaluating how big of an enhancement would the composites have if the fillers are aligned, and how much would adding more content of the fillers increment the thermal conductivity. A comparison between the thermal conductivities of the oriented composites and the unoriented was made. Results showed the aligned fillers had a better thermal conductivity and also that the more percentage of filler was added the higher the thermal conductivity would go. The synthetic graphite was the filler that enhanced the thermal conductivity the most, followed by the carbon fiber, and finally the carbon nanotubes, laser flash method was used for measuring the thermal conductivity.

Xu and Chung [27] performed thermal conductivity measurements on cement samples, which had silane and silica fume as admixtures. The silica fume used was first at 0% but then the following measurements were done at 15 % by weight of the cement. For the silane it was used first as 0%, and the % was increased to .2, .5, .75, 1, 1.5, and 2 % of the weight of cement. The thermal conductivity measurements obtained were given as a product of the thermal diffusivity, which was measured via laser-flash method. The silane and silica fumes showed to have an increase in thermal conductivity as high as 38%, since the thermal conductivity of the cement paste by itself was .52 W/mK, while with 15% silica fume and 2% silane showed a k value of .719 W/m-K. Showing the addition of these two admixtures increases the thermal conductivity, while the addition of the silica fume by itself decreased the thermal conductivity of the cement paste. The authors found that silane provides a network of covalent coupling among the silica fume particles, thereby increasing both the specific heat and the thermal conductivity, in addition to increasing the compressive strength and modulus and decreasing the compressive ductility.

Khedari et al. [28] developed a coconut coir which was used to develop a new type soil-cement block with low thermal conductivity. The thermal conductivity measurements were performed according to JIS R 2618, the measurements showed that increasing the content of coconut fiber made the thermal conductivity to be lower, different ratios of soil:cement:sand were used on the samples, but all of them ranged between .6 and 1 W/m-K, which when comparing to the literature showed a decrease of around 50%. The development of this new blocks could help to prevent heat transfer as well as saving energy.

Khedari et al. [29] felt the need to create a new lightweight composite for its use in construction, they evaluated eighteen coconut fiber specimens and 12 durian specimens, these specimens were prepared with different sizes of sand and mixing proportions (cement:sand:fiber). The thermal conductivity measurements were according to the JIS 2618 standard. While evaluating the thermal conductivity measurements, it was noted that the more fiber content the specimens have the lower the thermal conductivity would be. This was attributed to the short length of the fibers, because not only it makes them more difficult to align, but also the short length of the fibers leaves voids, that lead to the low thermal conductivity. Which is what the authors were looking for not only to create a lightweight composite, but also for it to have low thermal conductivity, these materials could be used for building roofs or walls.

Zha et Al. [30] prepared different types of samples: micro-Si₃N₄, nano-Al₂O₃, and micro-Si₃N₄-nanoAl₂O₃. The micro-nano sized samples showed better results on the thermal conductivity measurements, this was attributed because the co-filled model could easily form more compact thermal conductive channels. The thermal conductivity measurements were performed via HC-110 thermal conductivity tester.

Satyala et al. [31] fabricated bismuth telluride composites were prepared, the samples were embedded with silicon nano-inclusions, it was found that the thermal conductivity was dropped because of the silicon nano-inclusions, as the silicon content of the composites increased the thermal conductivity was dropped, the thermal conductivity measurements were performed via laser flash method.

Barucci et al. [32] made a comparison between the thermal conductivity of glass fiber, reinforced nylon against unfilled nylon, for these testings the method used to get the measurements was the longitudinal steady heat flow meter, when comparing the thermal conductivities, both k values increased as the temperature increased, however the glass fiber reinforced nylon showed very similar results as to the ones in the unfilled nylon. The authors found that glass fibre filling of nylon leads to a composite material with much greater dimensional stability. Instead, the low temperature thermal conductivity, remains very close to that of unfilled nylon.

Asako et al. [33] measured the thermal conductivity on compressed Japanese cedars, the unsteady hot-wire method was used to get the thermal conductivity. Thermal conductivity was evaluated in 3 directions, tangential (x), radial (y), and fiber (z) directions. The thermal conductivity of the tangential and fiber direction increased proportionally as the density of the Japanese cedars increased. This was attributed as the density increasing due to the compression, as for the radial direction it slightly increased as the density increased. This can be explained by considering both heat conduction in cell walls and cavity. The effect of air in the cavity on the effective thermal conductivity increases with the density increment.

Thunman and Leckner [34] evaluated the thermal conductivity of dry wood was evaluated, by using the hot-wire method to measure the thermal conductivity of the samples, it was concluded that there was a dependence between the thermal conductivity and the density of the material.

Barabash et al. [35] evaluated the irradiation results on different carbon fiber composites, what was found was that the thermal conductivity of the composites decreased after they were subjected to irradiation at 90 °C, however by annealing the samples at temperatures between 250 and 350 C, showed that the samples can partially recover their thermal conductivity. If the samples are subjected to more irradiation the drop in thermal conductivity is going to be even more. The authors recommend, in order to maintain the thermal conductivity of the samples, for the annealing to be done more frequently. The thermal conductivity values were obtained laser flash method.

Snead et al. [36] subjected two different types of carbon fiber composites to low-dose irradiation, which showed the carbon fiber composites to have a significant reduction on its thermal conductivity, in order to obtain the thermal conductivity, laser flash method was used.

Kalaprasad et al. [37] evaluated Different types of composites such as, sisal-reinforced polyethylene (SRP), glass-reinforced polyethylene (GRP) and sisal/glass hybrid fibre-reinforced polyethylene (GSRP). The thermal conductivity method used was the transient plane sources method. When comparing the results the pure LDPE as well as the SRP showed similar thermal conductivities, with the GSRP having a better k value peaking at .40 W/mk at 360C, and the GRP showed the best k values peaking at .50 W/mK at 360C.

Tavman and Akinea [38] measured the transverse thermal conductivity of HDPE . Which was reinforced with a chopped glass strand fiber mat. The method used to measure the thermal conductivity was the modified hot wire technique. Results found that as the % of glass was increased so did the transverse thermal conductivity, however as the temperature increased the thermal conductivity decreased. The authors determined that further testing was necessary since they only measured, pure HDPE, HDPE with 14% and 28% glass mat, further testing would help to find which is the optimal % of glass mat on the HDPE.

Gobbe et al. [39] made a study was made evaluating the use of two different methods to measure the thermal conductivity in order to use them in orthotropic media, one method is the hot-wire method, which gives the measurements of parallel or in-plane thermal conductivity, and the hot-strip method which measured the transverse thermal conductivity, the hot-wire method was performed on a stratified medium, and the hot-strip method was performed on a non-woven fibre insulator, which both methods rendering thermal conductivity results similar to the ones in literature, which means these methods can be used in orthotropic media.

Ren et al. [40] prepared two different samples: silica nanoparticle filled epoxy and silica nanofiber filled epoxy, an evaluated them to obtain which had the better thermal conductivity, they created an experimental setup (Figure 10) that consisted of a heater, a thin foil of indium, sample, another thin foil of indium, and a heat sink at the bottom. Two thermocouples were embedded in the indium foils to read the temperature across the sample. The data showed that the silica nanofiber filled epoxy has a higher k value, when compared with the silica nanofiber filled epoxy as well as pure epoxy, and results measured in literature.

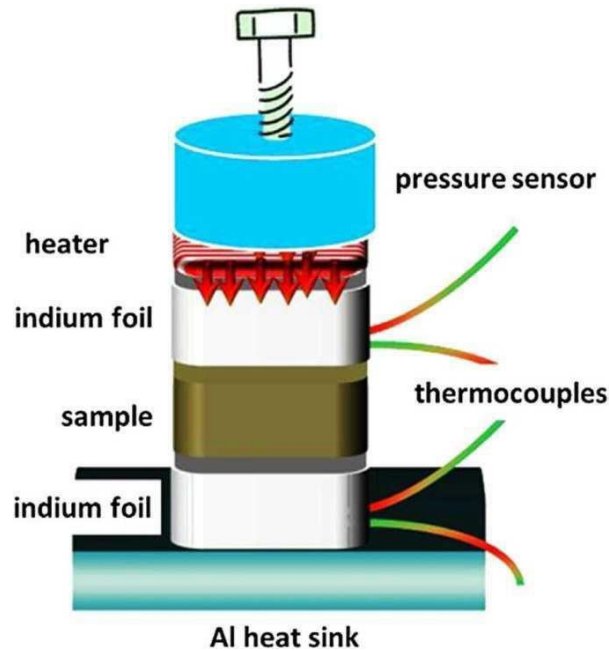


Figure 10. Schematic of the thermal conductivity setup [40].

Berbon et al. [41] fabricated thin C/SiC composites by slurry infiltration and pyrolysis, the thermal conductivity measurements were performed by laser-flash method. The samples were treated to temperatures as high as 1600 °C, and even though the samples treated around 1000 °C were perfect and without cracks, and the ones treated to 1600 °C had pores and cracks. Nonetheless, the latter ones had their thermal conductivity increasing considerably due to the exposure to higher temperatures during the heat treatment.

Agrawal et al. [42] evaluated the thermal conductivity of oil-palm-fibers on a phenolformaldehyde (PF) matrix, they prepared 4 different types of fibers, untreated, treated with alkali, treated with silane, and treated with acetic acid. The transient plane source technique was used to get the thermal conductivity measurements. Results concluded that the silane treatment as well as the alkali treatment enhance the thermal conductivity of the samples by

50%, while the treatment with acetic acid barely increased the thermal conductivity of the sample, staying almost the same as the untreated sample.

Gumen et al. [43] compared three different types of commercial ceramic fibers, which contained different percentages of aluminum oxide, VK-60, ABK-70, and VK-80, these fibers contained a diameter that ranged between 10 and 12 mm. The transient plane source (Figure 11) was used to measure these fibers. As the aluminum content increased in the ceramic fibers the thermal conductivity of the fibers decreased, while the insulation properties of the fibers increased. The VK-60 fibers had the greater thermal conductivity, while the VK-80 had the lowest value of thermal conductivity, .17 and .1 W/mK respectively.

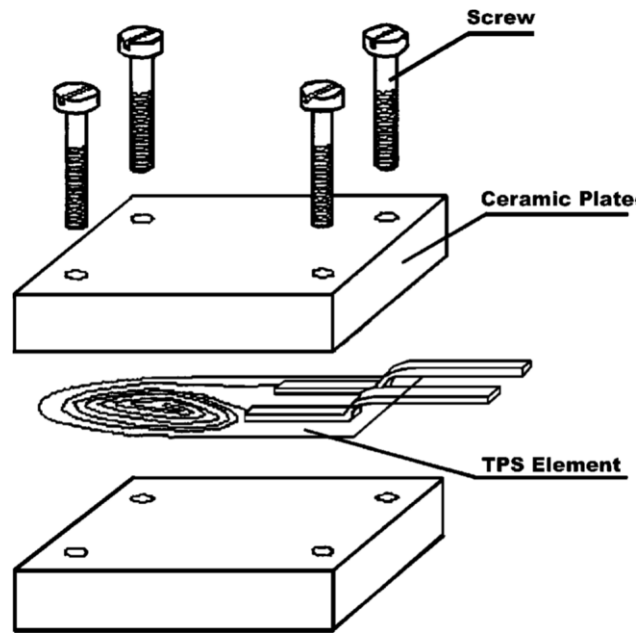


Figure 11. Schematic of the thermal conductivity setup [43].

Kanagaraj and Pattanayak [44] prepared plain fabric E-glass/Epoxy composites, they had fiber concentrations of 32.5%, 35.2%, 39.2% and 48.9% volume fraction. The thermal conductivity of these samples was measured by the guarded hot plate technique, it was found that the thermal conductivity of the samples increased as the temperature increased. The thermal conductivity increased as the fiber concentration increased, this later increments happened at a different rate depending on the temperature on which the thermal conductivity was being evaluated.

Bailleul et al. [45] performed the evaluation of the thermal conductivity of epoxy resin composite and Fiberglass reinforcement via an apparatus created by the authors (Figure 12). The thermal conductivity of the samples proved to be temperature dependent, however there was not a big enhancement of thermal conductivity with these composite.

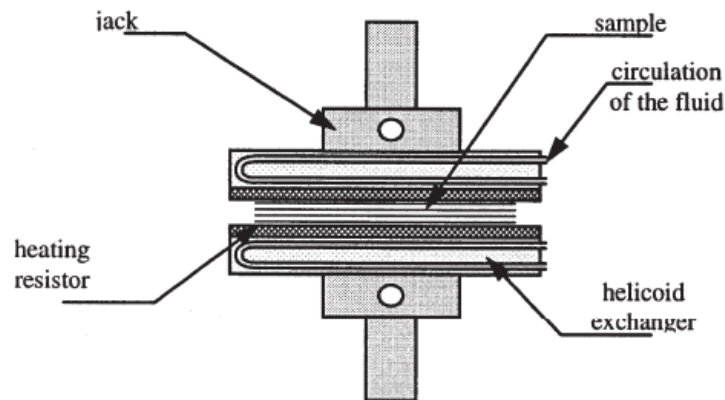


Figure 12. Schematic diagram of the experimental setup [45].

Lee and Choi [46] evaluated the thermal conductivity of epoxy silica matrix composites, with 0, 2, 4, and 6 wt% of titanium oxide added to the composites. The addition of titanium oxide did enhance the thermal properties of the epoxy silica composites, however the increase in

thermal conductivity was minimum. Adding more wt% percentage of titanium oxide has to be added to the composites, or reduce the quantity of silica and epoxy in the matrix, laser flash method was used to measure the thermal conductivity.

Gao and Zhao [47] prepared epoxy composites were prepared, which included micro-aluminum oxide particles. These composites had two different types of fillers at different wt%, and the fillers were graphene and carbon nanotubes. After comparing the results, even though the composites thermal conductivity increased as the temperature increased. The composites with graphene as a filler showed the best results. The thermal conductivity measurements were performed via hot disk thermal analyzer.

Donnay et al. [48] made epoxy-matrix composites, with boron nitride as a filler. The composites contained from 10w% up to 20w% of BN. The results obtained were the best ever recorded for an epoxy matrix with BN, $\sim 58 \text{ W/m}^2\text{K}$. The best results were obtained at 20wt%, hot disk thermal analyzer was used to measure the thermal conductivities.

Fu and Mai [49] evaluated short-fiber-reinforced polymer (SFRP) composites were evaluated via the guarded hot plate method. It was found not only that the thermal conductivity of the SFRP composites increases linearly with the fiber volume fraction, but also that the thermal conductivity increases with the length of the fibers. Also, the thermal conductivity decreases if the fibers are unaligned. The authors recalled that the last two effects would be highly dependent on the thermal conductivity of the fibers.

Li et al. created Te/Bi₂Te₃ core/Shell heterostructure nanotube (NT) composites with rough serrated surfaces were created. The thermal conductivity of the samples was measured via

laser-flash method. The thermal conductivities remained low even after raising the temperature up to 400 K, they remained stable from 300 to 400 K.

Stacy et al. [51] measured the thermal conductivity of aluminum nanoparticles, the procedure consisted on sieving the aluminum powder through a 325 mesh. Afterwards the sieved powder was pressed into cylindrical pellets. The thermal conductivity was measured via laser flash method. Results showed that as the density of the aluminum pellets increased so did the thermal conductivity. Starting from 0.2 W/m-K and reaching its highest measurement at 1 W/m-K at a density of 2.3 g/cm³.

Lee et al. [52] prepared tungsten-copper nanocomposites, with different wt% of copper ranging from 5 to 30 wt%. The thermal conductivity measurements were performed via laser flash method. Due to the high thermal conductivity of copper, as the wt% of copper increased in the sample the thermal conductivity was higher. For the samples with lower contents of copper did not have significant increments in their thermal conductivity as the temperature was raised.

Shen et al. [53] added a thin nano-size Molybdenum layer to diamond/copper composites. The Molybdenum added reacts with the diamond nanoparticles, causing the thermal conductivity of the samples to be doubled. The coating of Molybdenum causes the thermal boundary resistance to decrease, which causes the thermal conductivity to increase. Thermal flash method was used in order to obtain the thermal conductivities of the samples.

Harish et al. [54] made lauric acid based phase change nanocomposites, in order to enhance the thermal conductivity, graphene nanoplatelets were added. The thermal conductivity of the nanocomposites was measured via hot wire method. The experimental results showed, the thermal conductivity increasing considerably due to the addition of the graphene nanoplatelets.

When comparing the results obtained among the different samples, the graphene was shown to outperform metal nanoparticles, as well as carbon nanotubes.

Fang et al. [55] prepared nano-micro structure boron nitride and aluminum oxide epoxy composites. It was found that the design of the composite as well as the surface modification play important roles on the thermal conductivities of the samples. The increase of the fillers enhanced the thermal conductivity up to a certain point. As the temperature increased so did the thermal conductivity, laser flash method was used to measure the thermal conductivity of the samples.

Foley et al. [56] prepared sapphire substrates with nano-grained strontium titanate deposited on them. The film thermal conductivities were measured with a hot disk thermal analyzer. Results showed, that as the grain size from the strontium-titanate decreased, so did the thermal conductivity, the grains measured averaged from 30 to 90 nm.

1.2.4 Mats

Silva et al. [57] prepared several samples: low thermal conductivity samples (LTC) fabricated from a woven mat made of PAN-based carbon fibers and cured with epoxy. High thermal conductivity samples (HTC) made from a woven mat made of coal pitch-based carbon fibers and cured with epoxy, and unitape samples (UNI) fabricated from carbon fibers and cured with epoxy. The experimental setup (Figure 13) consisted of two steel plates with a sample clamp and five type-K thermocouples in each plate to estimate heat flow in and out of the samples. The measurements were calculated under two different power inputs (4.5 and 10.3 W) each test as run for 12 hours, first at 4.5 W and then at 10.3 W, until they reached steady state for 1 hour. The measurements for the LTC and HTC samples, it is shown that changing fiber angle, was an excellent way to increase the thermal conductivity of the samples tested.

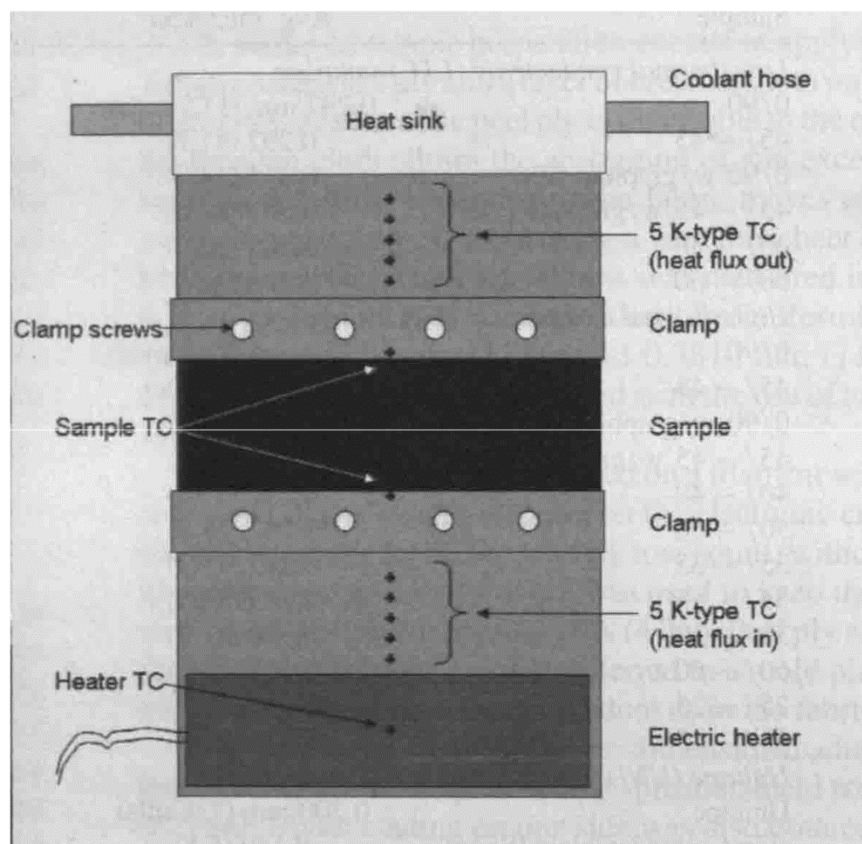


Figure 13. Schematic of the thermal conductivity setup [57].

Bing and Ying [58] made carbon nanofiber mats were via electrospinning method, the diameter of these mats varied between 220-1000 nm. When electrospinning these mats, during the analysis, they found out that the higher the supplied voltage (20kV) the smaller the fiber diameter would be (423nm) as well as the farther the spinning distance (20cm) the smaller the fiber diameter (423nm). The thermal conductivity was measured via Laser Flash method, it was found that the thermal conductivity decreases as the fiber diameter decreases, also the higher the temperature the higher the thermal conductivity will rise.

Nayandeeep et al. [59] made carbon fibers into ‘‘mat-like’’ materials at the National Composite Center, from these mats some were ungraphitized (heated around 1500 °C) and the rest were graphitized at 3000 °C. The in-plane and through-plane thermal conductivities were measured. Two different setups were used, for measuring the in-plane thermal conductivity the dual-mode heat flow meter was used, as for the through-plane thermal conductivity, the dynamic plane source was used. The results from the measurements are displayed on Figure 14. There is a big difference between the in-plane and through-plane thermal conductivities but this can be somewhat expected due to the anisotropic orientation of the nanofibers, on the other hand it can also be seen that the higher the volume fraction of nanofibers the higher the thermal conductivity will be, especially is the sample is graphitized.

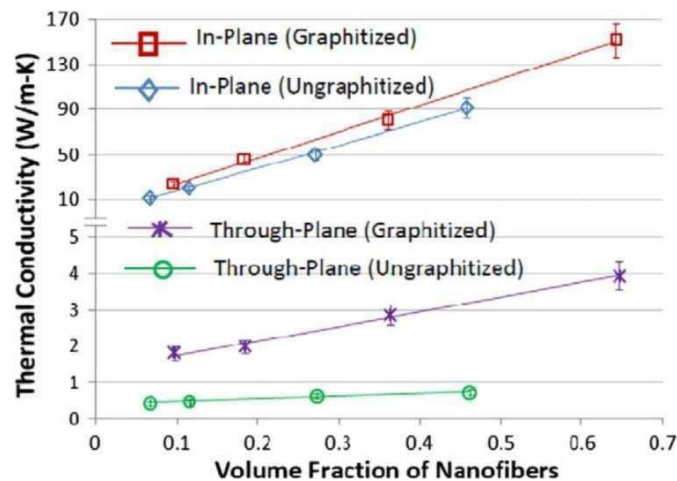


Figure 14. Thermal conductivity of mats as a function of the volume fraction of nanofibers [59].

Han et al. [60] added a Polyamic acid (PI) solution on which a pitch powder/N,N-Dimethylformamide suspension, nanofiber mats via electrospinning were made from this solution, which was subjected to heat treatment in a vacuum furnace under the temperature of 350°C for 45 minutes. These PI-Pitch blend nanofiber mats were subjected to thermal conductivity testing, in

order to measure the in-plane thermal conductivity, the dual-mode heat flow meter was used, as for the through-plane thermal conductivity, the dynamic plane source technique was used. The measured results, for the in-plane thermal conductivity, the thermal conductivity increased as the pitch content was increased, as for the through-plane measurements the addition of pitch initially did show increment on the thermal conductivity, but even though the content of pitch was increased, the thermal conductivity remained the same.

Park et al. [61] created carbon fiber mat/phenolic composites with different types of fillers were created, the modified transient plane source technique was used to measure the thermal conductivity of the samples, when evaluating the samples. It was determined that the carbon fiber mat/phenolic composites with aligned fibers showed a much higher thermal conductivity than the randomly aligned carbon fiber mat/ phenolic composites.

Xing et al. [62] prepared epoxy mats, with the addition of carbon nanotubes as well as copper nanowires. In order to improve the thermal conductivity of the epoxy. The carbon nanotube buckypaper and the copper nanowire mat were prepared separately, and were put together inside a filter and sealed. After the buckypaper and Cu nanowires mat were together, under vacuum the epoxy solution was added to flow through the thickness direction of the buckypaper and Cu nanowire mat. After several minutes the composites were taken out and merged together using a hot press machine, making the CNs/Cu nanowire/Epoxy composite mats. The viscosity of the epoxy solution was controlled in order to have a better handling of the percentage of CNs and Cu nanowire present on the composite mats. A DRL – III Thermal conductivity tester was used to measure the thermal conductivity of the samples. The thermal conductivity of the epoxy mats increases as the CNT/Cu content increases, it may not be a huge thermal conductivity measurement.

However, considering the low values of thermal conductivity epoxy has, when being subjected to an increment of the thermal conductivity of around 900%. Showing, that the inclusion of these fillers enhances the thermal conductivity of the mats.

Price and Jarratt [63] made different mats of PTFE they contained: PTFE, unsintered PTFE/glass fiber mats, and sintered PTFE/glass fiber mats. The sintered mats also contained different fractions of aluminum powder (5, 10, 15, and 30% respectively). The thermal conductivity measurements were performed by Lees disk method, which consists of three copper plates (A–C) drilled to accept liquid-in-glass thermometers and a 6 W electrical plate heater of the same diameter as the copper plates. After comparing the results it was concluded that sintering as well as the addition of Al powder increased the thermal conductivity of the samples. These increments could have been due to the change in crystallinity of the PTFE samples, or it could have also been because there was a better contact between the polymer and the glass, due to the voids being reduced.

1.2.5 Thin Films

Bullen et al. [64] measured the thermal conductivity of amorphous carbon film. The samples of amorphous carbon were prepared by two different methods: Remote-Plasma Chemical Vapor Deposition (RPCVD), by using this method the amorphous carbon acquired a soft, low density form. By Plasma Assisted Chemical Vapor Deposition (PACVD), the amorphous carbon acquired mechanical properties similar to the protective coatings of “diamond-like-carbon”. More samples were obtained, and were prepared by Filtered-Arc Deposition (FAD) here the properties were similar to what is called “tetrahedrally-bonded” amorphous carbon.

In order to measure the thermal conductivity, first a 10 μm wide Al line- Sputter was deposited on the surface of the thin films, where it was patterned by photolithography, this served as a heater as well as a thermometer during the measurements, which were performed by the 3ω method. They wanted to see the effect of sample thickness on their thermal conductivities. For samples with low thermal conductivities (the ones prepared from PRCVD and PACVD), the thermal conductivity was not affected by the change in thickness whereas the ones prepared by FAD were affected by the change in thickness.

Sweeting and Lui [65] performed an in-plane and through-thickness thermal conductivity test. The material used were commercial carbon-epoxy plain weave, the fiber volume present in these laminates was around 49%. The in-plane measurements showed that as the temperature increased so did the thermal conductivity, the highest temperature reported was 180 $^{\circ}\text{C}$ with a k value of 3 $\text{W/m}^{\circ}\text{K}$, as for the through-thickness measurements the results were the same with the k value slightly changing as the temperature increase, but it was around .65 $\text{W/m}^{\circ}\text{K}$ for most of the samples.

Kandare et al. [66] prepared nano-reinforced carbon/epoxy laminates, the thermal conductivity was measured via laser flash method. When performing the thermal conductivity measurements it was determined that the inclusion of thermally conductive nano-fillers enhances the through-thickness thermal conductivity, a 40% increment was shown comparing the thermal conductivity of the nano-reinforced against the non-reinforced laminates.

Kato et al. [67] used the Angstrom method to measure the thermal conductivity of different films (aluminum nitride, and aluminum oxide). The thermal conductivity measurements showed that as the thickness decreased, the in-plane thermal conductivity of the films increased, with the aluminum nitride having a thermal conductivity of 8.4 W/mK , and the aluminum oxide a

value of 4.5 W/mK, the thickness of the samples was .240 μm . Zheng et al. [68] prepared nanocrystalline bismuth antimony telluride thin films. Initially the thermal conductivity measurements were low, but were increased as the strain was shifted from compressive direction to the tensile direction. The thermal conductivity measurements were performed via omega 3 method.

Yan et al. [69] prepared boron nitride-coated multi-walled carbon nanotube films, it was found that with lower loading of boron nitride, the thermal conductivity was improved, laser flash method was used to obtain the thermal conductivity of the samples.

Donovan et al. prepared nano films of nano-grained barium titanate. It was found that as the grain size of the barium titanate decreases so will the thermal conductivity, and as the temperature increases so would the thermal conductivity, however there was more dependence on the grain size than temperature, the thermal conductivity was measured via time domain thermorefectance.

Tang et al. [71] developed a nano-porous thin film, on which the thermal conductivity was measured via laser-flash method. It was found that as the pore size increases the thermal conductivity decreases. The scattering boundary area has a significant effect on the thermal conductivity, the nano-pores are able to reduce the thermal conductivity due to phonon boundary scattering.

1.2.6 Carbon Nanotubes

Motoo et al. [72] attached a single carbon nanotube sample was attached to a T-type sensor, this T-type sensor is able to measure the thermal conductivity of a single carbon fiber, metallic

and nonmetallic wire, etc. This method is considered to have the advantages of simplicity and high accuracy. The thermal conductivity of a carbon nanotube increases as the diameter decreases while being tested at room temperature. This diameter-dependent thermal conductivity indicates that the interactions of phonons and electrons, with multiwalled layers affect the thermal conductivity of the sample, which results in thermal conductivity increasing as the number of multiwalled layers decreases. A single-walled carbon nanotube is expected to have much higher thermal conductivity.

Osman and Srivastava [73] measured the temperature dependence of the thermal conductivity of single wall-carbon nanotubes; they compared the different peaks of the SWNT by their aspect ratio (length/diameter). What they were able to find was that at 100K the SWNTs for all diameters had a similar value on their thermal conductivity. However, when the temperature went into higher temperatures. The thermal conductivity was higher with the SWNTs with a larger diameter, showing a temperature dependence. The reason for this behavior of the SNWTs was found that two different factors contribute to this: 1. the onset behavior of Umklapp scattering, which shifts to higher temperatures for nanotubes with larger diameters, and 2. the fact that heat is carried mainly through radial phonons.

Young et al. evaluated [74] The relationship of the individual multi-walled carbon nanotubes (MWCNTs) and their thermal properties, including the thermal conductivity among them. The authors, prepared 4 different MWCNTs mats (buckypaper); two of these buck yapers were from a commercial source, while the other 2 were synthesized by them. The thermal conductivity was measured via the Laser Flash method, after the thermal conductivity was evaluated, it was found that the thermal conductivity of the MWCNTs mat may depend of the different geometric properties of the MCWNTs, these properties are diameter, network length,

and total length, among many others. It was found that the in-plane thermal conductivity of the MWCNTs increases as the diameter of the samples is smaller, while as for the out-of-plane thermal conductivity, this will increase as the diameter of the samples is higher.

Tang et al. [75] doped carbon nanotubes were doped with different concentrations of cobalt oxide, the concentrations consisted in 0%, 1 wt%, 3wt%, and 6wt%, after the doping was performed, the mixtures were pressed into pellets, the thermal conductivity was measured with a physical property measurement system (PPMS) having temperatures ranging from 30 to 350K. When measuring the samples it was noted that even though the temperature increasing made thermal conductivity to rise, however the bigger the wt% the lower the thermal conductivity was, this was attributed to increasing phonon scattering.

1.3 Methods to Measure Thermal Conductivity

1.3.1 Guarded Hot Plate Method

This method is a steady-state method of heat flux measurement, here the thermal contact conductance between two 25 x 25 mm² copper blocks with a composite specimen between them is measured using the guarded hot plate method. The heat is provided from a copper block, which has two heating coils embedded to it, the temperature is regulated using a temperature controller. This copper block is in contact with one of the two 25 x 25 mm² copper blocks that have the composite specimen sandwiched. The cooling part is provided from another copper block, which has running water that flows in and out of the block. This block is in contact with the other 25 x 25 mm² copper block. The temperatures are measured when the system reaches a steady state. A steady state is assumed when the temperature varies between +/- 0.1 °C for 15 minutes.

The Guarded Hot Plate method chosen by Han Et. Al [7] is according to the ASTM Method D5470, which can be seen below in Figure 15.

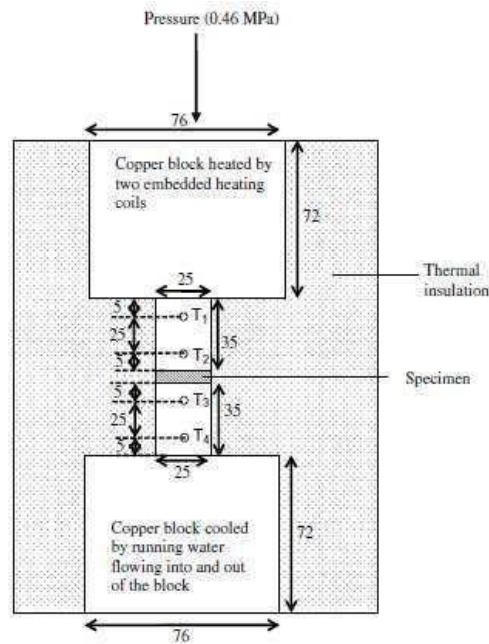


Figure 15. Guarded Hot Plate method set up for measuring thermal conductivity [7].

In order to measure the thermal conductivity, the heat flow is obtained by measuring by using the following formula:

$$Q = \frac{kA}{d_A} \Delta T \quad (1)$$

Where

A = cross – sectional area of the copper block (m^2)

d_A = distance between thermocouples T1 and T2 (mm)

k = thermal conductivity of copper ($W/m * K$)

ΔT = difference in temperature from thermocouples (K)

$$q = \text{heat flow } \left(\frac{W}{m^2}\right)$$

Afterwards the temperature of the top copper block (T_A) is calculated, by the following formula:

$$T_A = T_2 - \frac{d_B}{d_A} (T_T - T_2) \quad (2)$$

Where:

d_B = distance between thermocouples T_2 and the top of sample material

The temperature of the bottom copper block (T_D) is calculated, by the following

formula

$$T = T_2 - \frac{d_D}{d_C} (T_3 - T_4) \quad (3)$$

Where:

d_D = distance between thermocouples T_3 and the bottom of sample material

d_C = distance between thermocouples T_3 and T_4

Finally the thermal resistivity (θ) is calculated from the equation:

$$\theta = (T_A - T_D) \frac{A}{Q} \quad (4)$$

The thermal conductivity of the sample material is measured as the inverse of the slope of the curve of the thermal resistivity vs thickness.

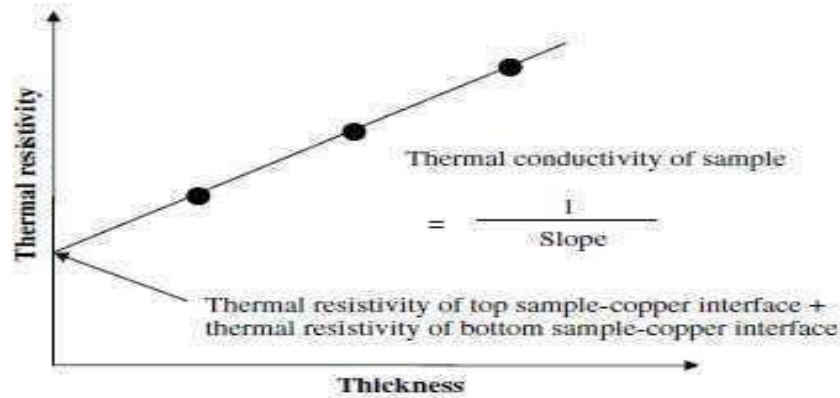


Figure 16. Schematic explaining the linear dependence of the thermal resistivity on the specimen thickness [7].

1.3.2 Laser Flash Method

The laser flash method consists of the following steps: A sample is positioned on a sample holder, located in a furnace. The furnace is then held at a predetermined temperature. At this temperature the sample surface is then irradiated with a programmed energy pulse (laser or xenon flash). This energy pulse results in a homogeneous temperature rise at the sample surface. The resulting temperature rise of the rear surface of the sample is measured by an IR detector and thermal diffusivity values are computed from the temperature rise versus time data. The resulting measured signal is used to compute the thermal diffusivity.

A machine that does the laser flash method is the Ulvac laserPIT, which uses the Angstrom method of AC periodic scanning laser heating to measure the in plane thermal diffusivity of thin materials and deposited films.

The Angstrom method consists of determining the thermal conductivity of a metal rod by applying an alternating heat pulse to one end while leaving the other end at room temperature. Doing this causes a heat wave to propagate down the rod and creates an observable temperature difference between two points on the rod. This also creates a varying phase relationship between the measured temperature recorded at the first and second points. The thermal conductivity of the rod can be determined if the temperature of these two points is measured as a function of time.

The thermal conductivity is calculated from the thermal diffusivity (D) using the equation:

$$k = D C_p \rho \quad (2)$$

Where

$$k = \text{thermal conductivity (W/m * K)}$$

$$D = \text{density } \left(\frac{\text{kg}}{\text{m}^3}\right)$$

$$C_p = \text{specific heat } \left(\frac{\text{J}}{\text{kg} * \text{K}}\right)$$

$$\rho = \text{thermal diffusivity } \left(\frac{\text{m}^2}{\text{s}}\right)$$

The issue with this method is that, when compared to other methods laser flash does go to much higher temperatures, but it does not reach the required thickness since its smallest it measures is around 100 nm.

1.3.3 Microfabricated Device

The microfabricated device was developed by Shi [76], this method consists in: an individual nanowire thermally connects 2 suspended microfabricated microstructures, as shown in

Figure 17, the suspended microstructure consists of 2 silicon nitride (SiN) membranes each suspended by 5 Si beams that are $420\ \mu\text{m}$ long and $.5\ \mu\text{m}$ thick. A thin platinum (Pt) resistance coil (serpentine line) and a separate Pt electrode are patterned onto each membrane; each resistor is electrically connected to 4 contact pads by the metal lines in the suspended legs, also they can serve as a heater to increase the temperature of the suspended microstructures, as well as a resistance thermometer to measure the temperature on each microstructure. When a dc current (I) was supplied to one Pt RT to raise the temperature of one membrane, part of the joule heat generated in the heating membrane, was conducted through the nanofiber to the other membrane.

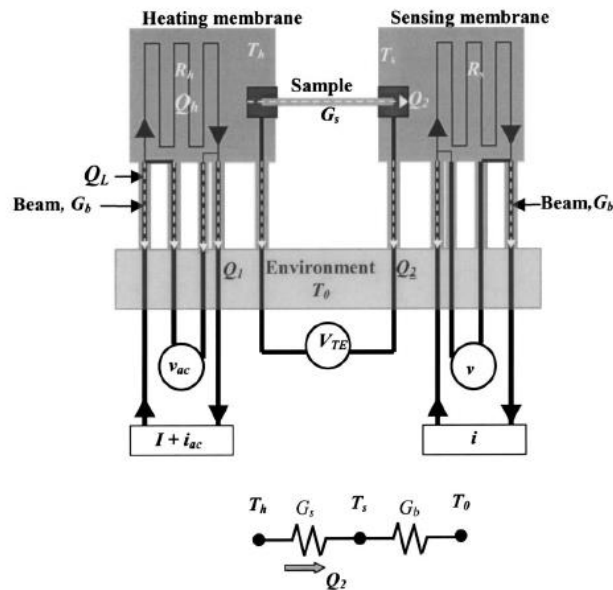


Figure 17. Microfabricated device [76].

When measuring these nanofibers, two different sampling methods were used: one was wet deposition method, where a solution containing the nanofibers is dropped and spun on a wafer containing many suspended devices. It was found that the nanostructures are often absorbed on the 2 Pt electrodes.

The other method was Chemical Vapor Deposition (CVD) to grow individual Single Walled Carbon Nanotubes (SWCNT) bridging the two membranes, they spun different solutions containing nanoparticles made of Fe, Mo, and Al_2O_3 . The suspended micro device is then placed in a 900C CVD tube with flowing methane, resulting in individual SWCNTs grown between two catalyst particles on the two Pt electrodes.

In order to measure the thermal conductivity, the following formula was used:

$$k = G_s L/A \quad (3)$$

Where

$$A = \sum_j^n \pi d_j \delta = n\pi\delta[d_1 + (n - 1)\delta] \quad (4)$$

And

$$G_s = \frac{Q_h + Q_L}{\Delta + \Delta T_s} \frac{\Delta T_s}{\Delta T_h - \Delta T_s} \quad (5)$$

Where

$$G_s = \text{Thermal Conductance of the sample } \left(\frac{W}{K}\right)$$

$$L = \text{Suspended length of the sample (m)}$$

$$A = \text{Cross - sectional area (m}^2\text{)}$$

$$n = \text{number of shells}$$

$$d_j = \text{diameter of the } j - \text{th nanotube shell (m)}$$

$$\delta = \text{interplanar spacing of graphite}$$

$$Q_h = \text{Joule heating in the heating Pt serpentine (W)}$$

$$Q_L = \text{Joule heating in one of the two Pt leads}$$

$$\text{supplying the dc current (I) to the heating serpentine (W)}$$

$$T_h = \text{Temperature rise in the heating membrane (K)}$$

$$T_s = \text{Temperature rise in the sensing membrane (K)}$$

When checking the results, they found they were able to get good readings for the thermal conductivity, however when comparing the results to the bulk, the measured results were lower. This

was mainly attributed to phonon-boundary scattering rate, phonon-defect scattering, this problem was a common reoccurrence when using the microfabricated device [77].

1.3.4 Kohlrausch Method

Kalnin built a test apparatus by the Kohlrausch method [78], in this procedure a test specimen is heated by electrical current until it reaches steady state. The heat applied on the sample flows from the center of the sample to both ends of it, the temperature on both sides is maintained thanks to a heat sink on each side, and in this case the heat sink is a copper clamping block. The setup is explained below on Figure 17.

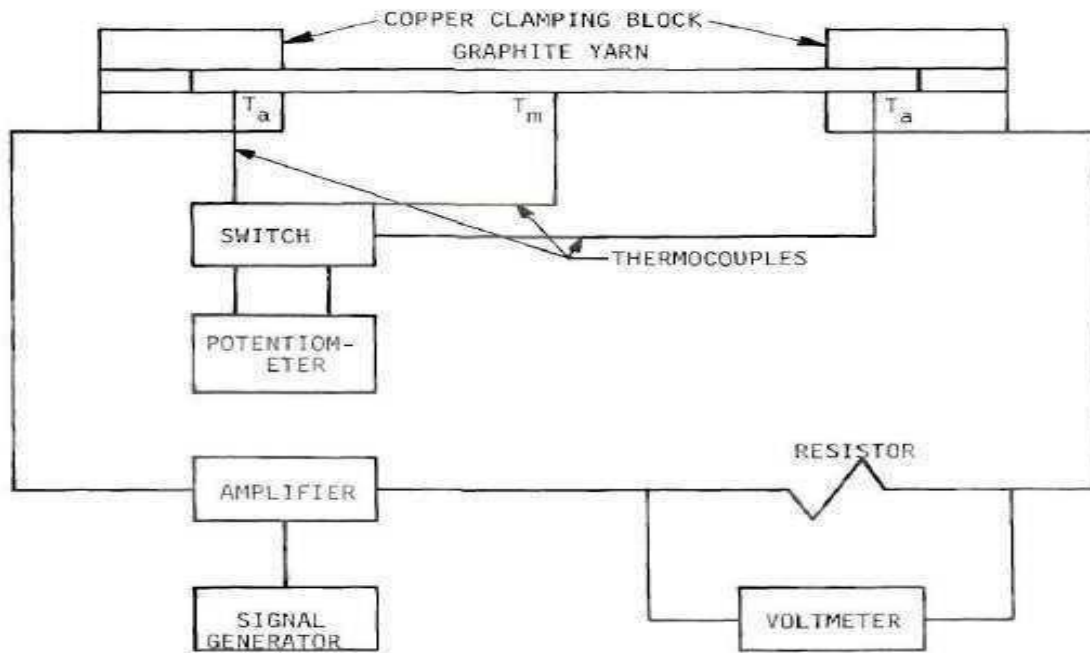


Figure 18. Experimental setup for the Kohlrausch method [78].

Before calculating the thermal conductivity, two conditions have to be known, the potential drop across the specimen, as well as the electrical resistivity.

After fulfilling these conditions the thermal conductivity can be calculated from the following formula:

$$k = \frac{\Delta e^2}{8R_e(T_m - T_a)} \quad (6)$$

Where

$$k = \text{thermal conductivity } \left(\frac{\text{W}}{\text{m} \cdot \text{K}} \right)$$

$$\Delta e = \text{potential drop across the specimen } (\Omega)$$

$$\rho_e = \text{electrical resistivity } (\Omega \cdot \text{cm})$$

$$T_m = \text{temperature at the center of the specimen (K)}$$

$$T_a = \text{temperature at the ends of the specimen (K)}$$

The Kohlrausch method can be considered as an indirect method for measuring thermal conductivity, since the electrical resistivity and surface emissivity have to be known prior to calculating the thermal conductivity, this method is suited from a very long test specimen, and is not a useful setup for low resistance fibers.

1.3.5 Hot-Wire Method

The hot wire method allows to measure the thermal conductivity utilizing a particular heat conduction equation 7), this method was found in previous articles [79] [80] measuring carbon fiber sample, in both cases the hot wire was used as a T type method, as shown in Figure. ,where a wire served as a heating source as well as a thermometer, with this T type method, the thermal properties of the hot wire were measured.

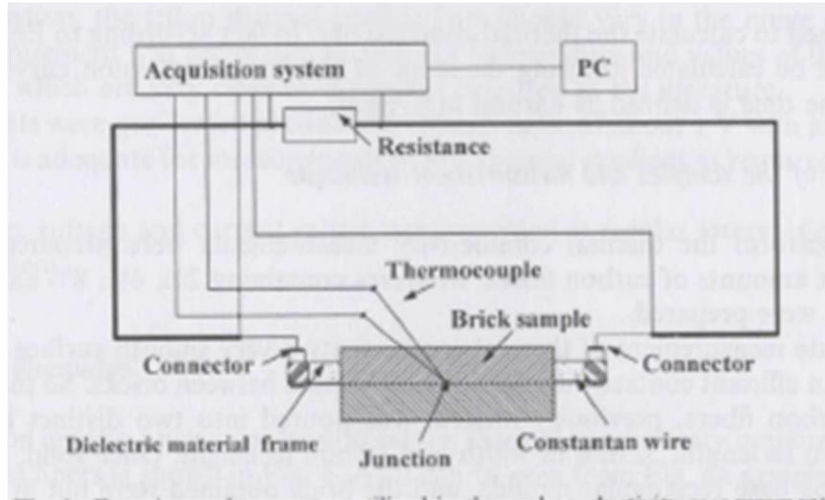


Figure 19. Hot wire setup [79].

The hot wire setup consists of: the hot wire welded with a thermocouple, a measuring circuit that includes a power supply, a rectangular frame of dielectric material, which helps to connect the hot wire, a high precision standard electric resistance and a controller data acquisition system. The formula for calculating the thermal conductivity is the following:

$$K = \frac{\left(\frac{VI}{4\pi L}\right)}{\left(\frac{dT}{d(\ln r)}\right)} \quad (7)$$

Where:

$$k = \text{thermal conductivity} \left(\frac{W}{m * K}\right)$$

$$V = \text{voltage (V)}$$

$$I = \text{current (A)}$$

$$L = \text{hot wire length (m)}$$

$$T = \text{temperature (K)}$$

$$t = \text{time (s)}$$

1.3.6 Non-Contact Optical Based Technique

Balandin et al. [81] discovered a non-contact optical technique. Measurements of the thermal conductivity of graphene were made using the confocal micro-Raman spectroscopy. The Raman spectroscopy-based measurement of the thermal conductivity is not suitable for the bulk crystalline materials with the high thermal conductivity because of the rapid escape of heat, produced by the laser excitation, in three dimensional systems. The latter prevents a local temperature rise detectable with the Raman spectroscopy for reasonable excitation power levels. Luckily, graphene has a thickness of only one atomic layer. Thus, graphene is suspended over a trench and heat in the middle, the heat is forced to propagate in-plane through the layer toward the heat sink. The extremely small cross-section area of the heat conduction channel makes the detection of the local temperature rise possible. The thermal conductivity is measured by the following formula:

$$k = \left(\frac{T}{2\pi r h}\right)(\Delta P/\Delta T) \quad (8)$$

Where:

$$k = \text{thermal conductivity} \left(\frac{W}{m * K}\right)$$

h = single layer graphene thickness (m)

ΔP = changing heating power (W)

ΔT = local temperature rise (K)

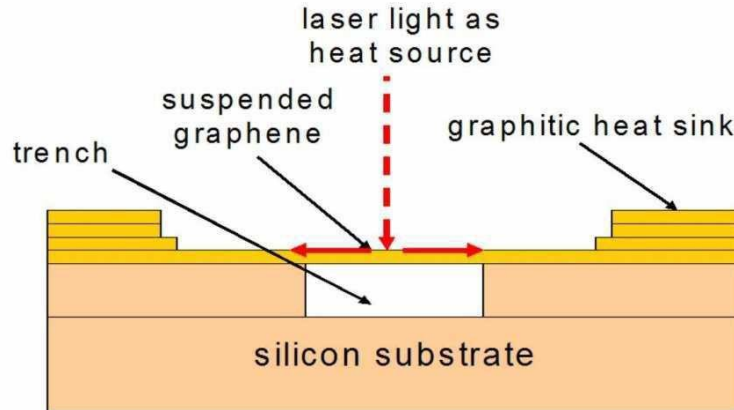


Figure 20. Non-contact optical based technique schematic [81].

1.3.7 Dual Mode Heat Flow Meter

The setup for the dual heat flow according to Mahanta et al. [82], consists in having a thin specimen in line and contacting a reference material of a similar width, held together by kapton tape, the setup is shown on Figure. This experimental setup helps to measure the in-plane thermal conductivity, accurately and reliably. If the material tested has a very small thickness (in nano- or micrometers), this method can get affected significantly by the heat loss due to convection. Therefore, if the material that is going to be tested is thin, the heat loss can be prevented to a minimum by having the setup run under vacuum conditions.

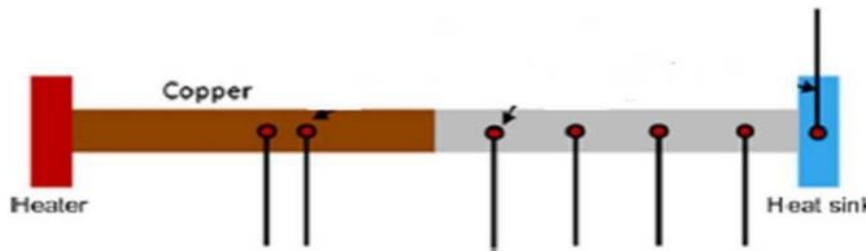


Figure 21. Dual mode heat flow meter [82]

The setup was done inside between clamps mounted on two end supports and then placed inside a bell-jar vacuum chamber. The reference sample, on this experiment was copper, was heated by two strip heaters located above and below the reference sample. The stainless steel base plate located inside the vacuum chamber acted as a heat sink, since it was in thermal contact since it was clamping the end of the sample. The reason the stainless steel base plate can be used as a heat sink is because of its high thermal capacity, when being compared to the sample it is clamping. The temperature was obtained from the measurement of 8 thermocouples: two thermocouples were located on the reference material, four were located at the sample, one was measuring the temperature on the heat sink, and the other was attached to the bell-jar, in order to measure the ambient temperature. It should be noted that the thermocouples located at the reference sample were apart from each other by 3 mm, and this was also the same for the thermocouples located on the tested sample. Once the setup was ready, testing on the duel flow heat meter was performed, and the thermal conductivity was calculated by the following formula

with steady-state temperature measurements:

$$k = \frac{d^2T}{dx^2} - \frac{h_r P}{A} (T - T_\infty) \quad (9)$$

Where:

$$k = \text{thermal conductivity } \left(\frac{W}{m * K} \right)$$

$$T = \text{temperature (K)}$$

$$x = \text{direction of conduction of heat transfer}$$

$$h_r = \text{coefficient of radiation heat transfer from sample}$$

$$P = \text{perimeter of sample (m)}$$

$$A = \text{area of cross - section of sample (m}^2\text{)}$$

$$T_\infty = \text{ambient temperature (K)}$$

Table 2. Comparison between the different thermal conductivity setups

Method	In-plane	Through-plane	Vacuum	Pros	Cons
Guarded Hot Plate	X	X		Reliable method and its done according to ASTM standard	Thermal conductivity is obtained from the thermal resistivity
Laser flash method	X		X	Thickness of the material can go as low as 100 nm	Expensive machine
Microfabricated device	X		X	Modern setup, very interesting method, measures nanowires.	Only measures a single fiber, phonon-boundary scattering rate, phonon-defect scattering, this problem was a common reoccurrence when using the microfabricated device
Kohlrausch method	X			Measures high thermal conductivity materials	Can only measure high thermal conductive material, since k depends on the electrical resistivity.

Hot-wire method	X		X	Gives accurate results, thanks to the controller data acquisition system	Depends on voltage
Non-contact optical based technique	X			Measures wide range from materials, from low thermal conductivity up to high thermal conductive materials such as graphene	
Dual mode heat flow meter	X		X	Does not depend on material specific dimensions, or meet specific limitations placed due to thermal resistance of tested samples. Thermal conductivity measurement only depends on the heat flow.	When measuring the temperatures of the reference and experimental samples, the averages are taken from both samples, instead of the difference in temperature, due to the high number of thermocouples.

CHAPTER II

EXPERIMENTAL SETUP

In order to design of the experimental setup, a study of literature was performed among the different apparatuses to measure thermal conductivity of both insulators and conductors. An apparatus was built to meet the need of measuring non-woven nanofiber mats.

The configuration of the experimental setup consisted on having a test specimen with an unknown thermal conductivity (~13 mm x ~50 mm. width x length) attached at one end of a reference material with known high thermal conductivity, for this instance copper was used as the reference material. The unknown and reference samples were attached together by a piece of copper tape. A part of the reference sample was placed inside two rounded strip heaters connected to an adjustable power supply. Two aluminum brackets were manufactured; one was made as a holder for the flexible heaters where the part of the reference sample would be inside, the other aluminum piece was used as a heat sink for the unknown material.

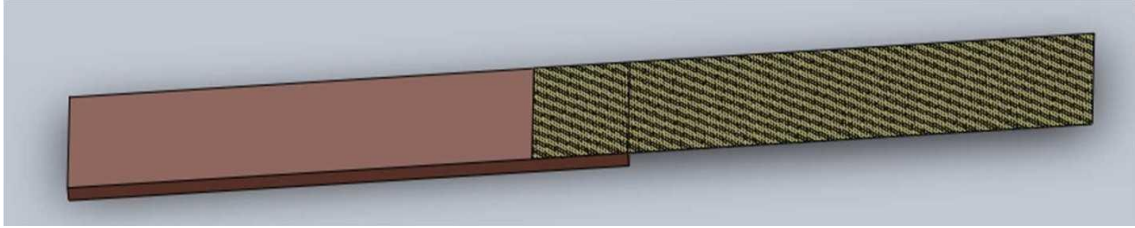


Figure 22. SolidWorks model of the copper material and the unknown material, for this instance carbon fiber.

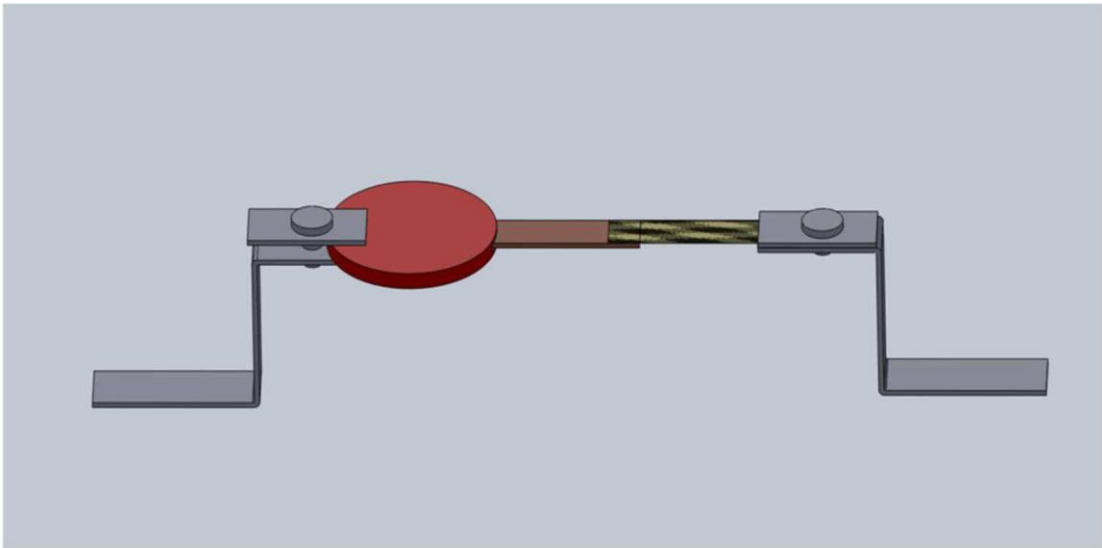


Figure 23. SolidWorks model of the thermal conductivity test setup

The aluminum pieces were mounted to an aluminum plate (18"x18"x0.5") which acted as a base of the vacuum chamber. The base of the aluminum brackets were fixed to the base by slotted holes, which allow for an adjustment of the test section for variable lengths of test specimen. All of the measurements were performed at vacuum setting inside a bell jar (12"x12"x0.5"), in order to prevent the effect convection losses which can be a significant problem for a thin mat of nanofibers.



Figure 24. Aluminum plate where the setup was mounted



Figure 25. Acrylic bell jar (12"x12"x0.5")

The temperature measurements were done by 4 thermocouples; 2 of the thermocouples were attached to the reference sample, while the remaining 2 were attached to the test sample. The thermocouple wires were mounted on base of the vacuum chamber using feedthroughs made of 1/8" copper tubes, which were filled with epoxy in order to prevent air leakage once a vacuum is created inside the bell jar. Feedthroughs were locked inside 1/8" compression fittings, which then were attached to the aluminum base.



Figure 26. Thermocouple inside the feedthrough and compression fitting.

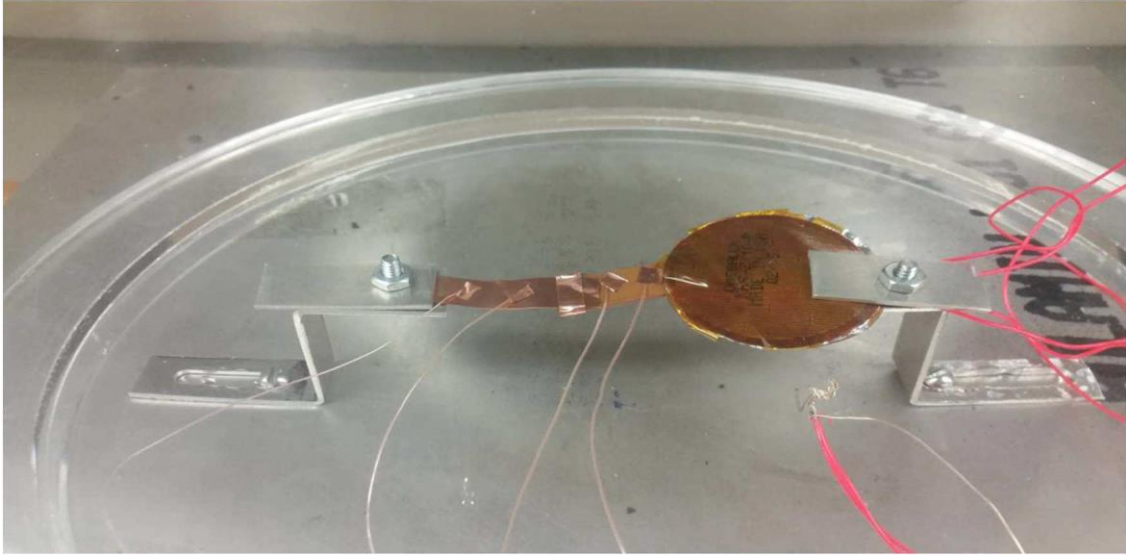


Figure 27. Copper foil being measured by the thermal conductivity tester

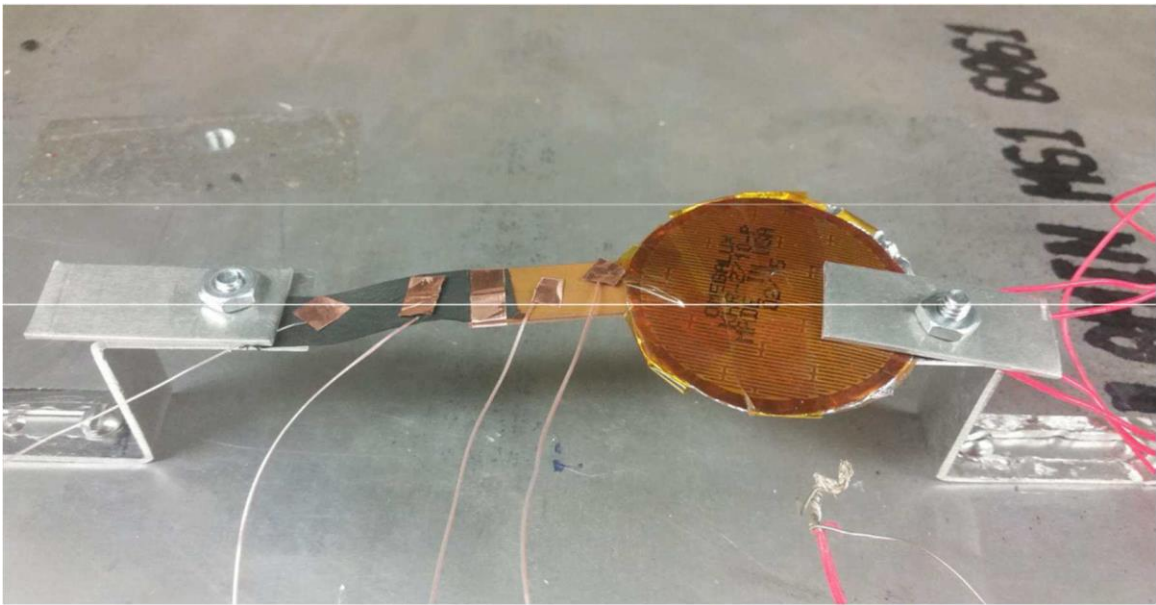


Figure 28. Carbon nanofibers being measured by the thermal conductivity tester.

CHAPTER III

RESULTS AND DISCUSSION

Before performing any measurements, the thermocouples were calibrated inside a temperature controlled water bath. Temperatures from the thermocouples was recorded after they reached a steady state; this was repeated for a range of 25 to 40 °C with an increment of 1 °C.

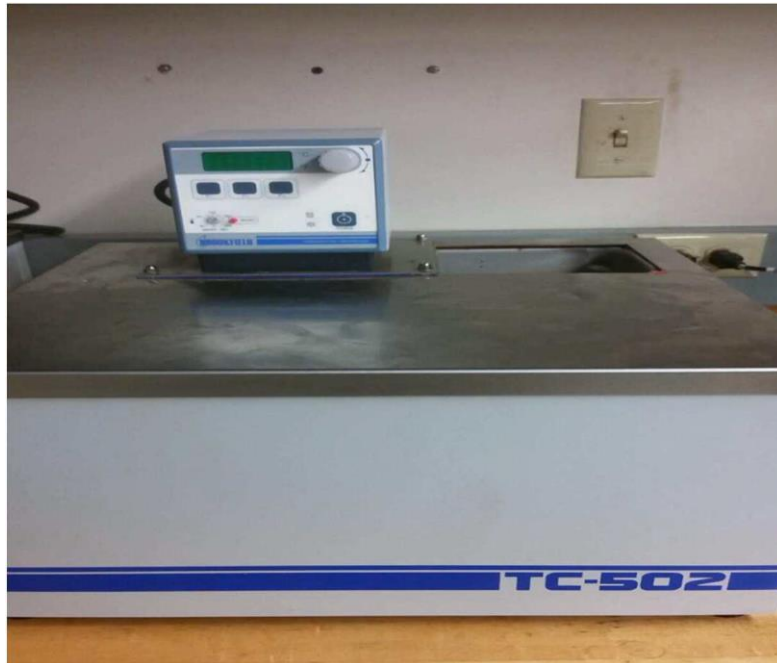


Figure 29. Thermostatic water bath used for thermocouple calibration

As the thermal conductivity of the material was being tested, the temperatures from the samples would be recorded once they reach steady state. The thermal conductivity is calculated using the following equation:

$$k_s = k \frac{\Delta T}{\Delta T_s} \frac{\Delta X_s}{\Delta X} \frac{Ac}{Ac_s} \quad (10)$$

The path used in order to obtain the equation goes as follows:

First the heat flux from the reference material was measured by the formula:

$$q'' = -k \frac{dT}{dx} \quad (11)$$

Where k is the thermal conductivity of the material, dT is the temperature difference between the thermocouples, T_1 and T_2 , which are the thermocouples located in the reference sample, and dx equals the distance between the thermocouples. This equation can also be written

as:
$$q'' = K \frac{T_1 - T_2}{\Delta x}$$

Afterwards, the heat transfer rate of the material is measured by the formula:

$$q = q'' Ac \quad (12)$$

Where q'' equals the heat flux and Ac is the cross sectional area of the reference sample, this formula can be rearranged as: $q = K \frac{T_1 - T_2}{\Delta x} (wt)$

In order to calculate the thermal conductivity of the experimental sample, the following equation is used which indicates the heat transfer rates are same for both reference and test samples:

$$q = q''_s A c_s \quad (13)$$

Which can be written as:

$$q = K_s \frac{T_3 - T_4}{\Delta x_s} A c_s \quad (14)$$

After isolating k_s , we arrange the equation and what we obtain is:

$$k_s = \frac{q \Delta x_s}{(T_3 - T_4) A c_s} \quad (15)$$

Finally equation (12) is inserted on equation (15), what is achieved is the final equation shown below as:

$$k_s = k \frac{\Delta T}{\Delta T_s} \frac{\Delta X_s}{\Delta X} \frac{Ac}{Ac_s}$$

Before performing any measurements with the sample materials, a validation of the thermal conductivity setup had to be made, by measuring the thermal conductivity of standard materials with known thermal conductivity and comparing the results with the ones in the

literature. PVDF was used to validate the low thermal conductivity measurements, while aluminum and copper were used to validate high thermal conductivity measurements. The results, shown below on Table 3, closely match the ones reported on literature, which validates measured thermal conductivities both high and low thermal conductive materials.

Since the known values were measured by the setup, the experimental uncertainty was calculated based on a standard uncertainty analysis procedure explained by Coleman and Steele

[75], by considering a general case in which a calculated value, r , is a function of J variables X_i :

$$r = r(X_1, X_2, \dots, X_j) \quad (16)$$

This equation represents a data reduction determining r from the measured values of the variables X_i . For a functional relationship given as equation (7), the experimental uncertainty in the result is given by:

$$U_r = \left[\left(\frac{\partial r}{\partial X_1} UX_1 \right)^2 + \left(\frac{\partial r}{\partial X_2} UX_2 \right)^2 + \dots + \left(\frac{\partial r}{\partial X_j} UX_j \right)^2 \right]^{\frac{1}{2}} \quad (17)$$

K is a function of temperature the X equals the different values that were measured. UX_1 being the uncertainty for X_1 , and the same goes for the remaining values of X . That's how the uncertainty is measured. $r = K$, being the function of what its measured, the partial derivative of K is taken in function of x . The values for uncertainty were analyzed, obtaining .058 for the temperatures (K) measured from the thermocouples, and .0005 for the distance (m) between the thermocouples.

Table 3. In-plane thermal conductivity of known materials by using the thermal conductivity setup

Material	Measured k value(W/m*K)	Measured k value in literature (W/m*K)
PVDF PURE	0.253 ±0.010	.19-.22
Aluminum A360	107.349±4.43	113
Copper	388±10.88	388

When the validation of the thermal conductivity setup was made, the sample materials were tested. The samples closely matched the dimensions previously mentioned, (~13 mm x ~50 mm. width x length). However, the thickness of the material was different for each of the samples. Samples 1-6 were from various PVDF-based material used for the validation of the thermal conductivity setup. These PVDF material were obtained from NASA, who wanted to know the thermal conductivity of their samples. The difference between the samples, was that each of the 3 samples had boron nitride along with different undisclosed materials. The thermal conductivity of the samples increased as the concentration increased, with the PVDF CCS100 samples showing the best thermal conductivity values.

Table 4. PVDF samples thermal conductivity measurements

Sample	Material	Measured k value (W/m*K)
	PVDF PURE	.253
1	PVDF NX10 20wt%	.419
2	PVDF Pt110 20wt%	.484
3	PVDF CCS100 20wt%	.531
4	PVDF NX10 40wt%	.824
5	PVDF Pt110 40wt%	.868
6	PVDF CCS100 40wt%	.963



Figure 30. PVDF Sample

Table 5. displays different types of poly(vinyl alcohol) (PVA) samples. The preparation of the samples goes as: A PVA nanofiber mat is prepared via the Forcespinning method, after the mat is successfully built, the next step is to precarbonize the samples under an acid treatment, such as samples 7 and 8 which were the pre-carbonized PVA samples. Finally the pre-carbonized samples are subjected to heat treatment at a temperature of 800 °C at a ramping rate of 3C/min. The carbonized PVA sample (sample 9) showed an increment of almost 10 times the thermal conductivity the pre-carbonized mats had. Meanwhile samples 13, 14, and 15 were carbonized PVA samples, but there was the desire to see how fillers would affect the thermal conductivity of the carbon fibers. After the carbonization one of the samples was doped with nitrogen (sample 13), and 2 other samples were coated with silver and copper respectively (samples 14 and 15). When comparing the results among the different carbon fibers, the doping the carbonized PVA with nitrogen did not increase the thermal conductivity significantly. On the other hand coating the samples proved to be a better alternative to enhance the thermal conductivity, since the silver and copper coating worked well on increasing the thermal conductivity. Especially the carbonized PVA with copper coating which showed an increment of 50% compared to the thermal conductivity of the carbonized PVA.

Table 5. PVA samples thermal conductivity

Sample	Material	Measured k value(W/m*K)
7	PVA Pre-carbonized #1	7.89
8	PVA Pre-carbonized #2	8.58
9	PVA Carbonized #1	71.6

13	PVA Carbonized Nitrogen Doped	78.2
14	PVA Carbonized Silver Coated	93.0
15	PVA Carbonized Copper Coated	159.1



Figure 31. Carbonized PVA sample

Meanwhile, when making a comparison between the fully carbonized PVA samples, there is a slight difference in the thermal conductivity between samples 9-12. Different factors can be attributed to the difference between the thermal conductivities. The most important one being that sample 9 and samples 10-12 were prepared at a different time, which is something to consider, because even though the method of preparation of the nanofiber mats was the same, there was an difference between the thermal conductivity of the mats. Among these reasons of the difference in the thermal conductivities could be one of the following: the fibers being shorter, broken or not being fully aligned in the radial direction, which prevents the heat flow to be ideal within the sample.

Table 6. Thermal conductivity of the PVA carbonized samples

Sample	Material	Measured k value(W/m*K)
--------	----------	---------------------------

9	PVA Carbonized #1	71.6
10	PVA Carbonized #2	78.7
11	PVA Carbonized #3	78.7
12	PVA Carbonized #4	81.6

Finally two copper foils which were bought from Omega were measured. Since the value of the foils were unknown, and the values recorded in literature which can range from 350~400 W/m*K, when performing the thermal conductivity measurements, they were found to be within the desired range.

Table 7. Thermal conductivity of the copper foil samples

Sample	Material	Measured k value(W/m*K)
18	Copper Foil #1	363
19	Copper Foil #2	363



Figure 32. Copper foil

When observing the relationship between the sample thickness and its thermal conductivity, the carbonized PVA Samples 1-4 have a similar thickness. However there is a difference between the thermal conductivity of the samples. This can help solidify the idea that perhaps the difference between the thermal conductivity of the samples, can be due to imperfections on the fibers, such having some of the fibers being short, or broken. Having a pristine carbon fiber mat, would be something very difficult to obtain, since there is always going to be defects, however we can assume the samples 2-4 had less imperfections than sample 1. Meanwhile, it cannot be safely assumed that the materials with the lower thickness have the greater thermal conductivity, or vice versa, since the two samples with those qualities do not show the highest thermal conductivity. The PVA carbonized copper coated sample has similar thickness to the PVA carbonized samples, however the thermal conductivity is higher than the samples due to the copper coating. Sample preparation it's a very important detail, because it can impact the thermal conductivity of the material, while the thermal conductivity mainly depends on the material type, when working with fibers, the preparation and fiber conditions do affect the thermal conductivity

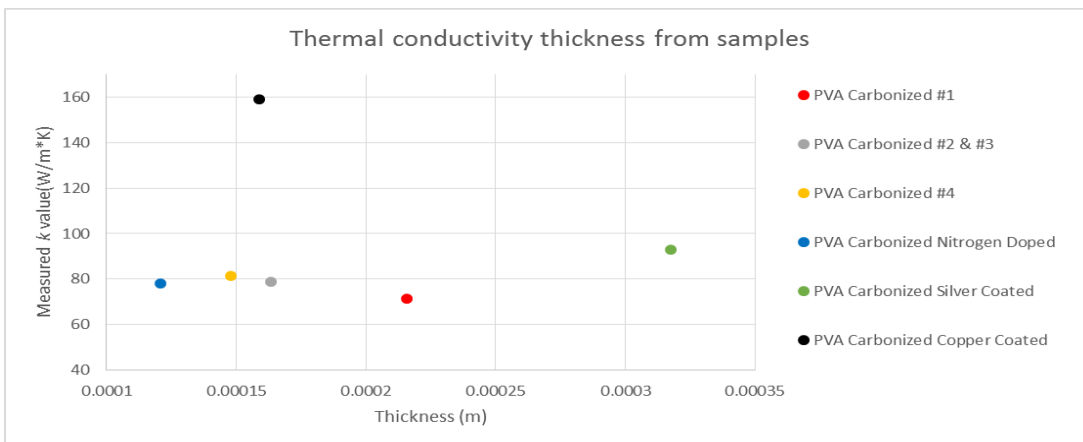


Figure 33. Comparing the relationship between the sample thickness and its thermal conductivity

Table 8. Thickness and thermal conductivity comparison of the sample material

Sample	Material	Measured k value(W/m*K)	Thickness (m)
9	PVA Carbonized #1	71.6	0.0002159
10	PVA Carbonized #2	78.7	0.0001635
11	PVA Carbonized #3	78.7	0.0001635
12	PVA Carbonized #4	81.6	0.0001478
13	PVA Carbonized Nitrogen Doped	78.2	0.0001207
14	PVA Carbonized Silver Coated	92.9	0.0003175
15	PVA Carbonized Copper Coated	159.0	0.0001588

Finally, the area density of the sample materials was calculated by evaluated the areas as well as the mass of the material, this will be helpful because in the event the material is pressed, the thickness change, however the density are should remain the same. If a comparison is made between the area density and the thermal conductivity, the samples the density above .1, which were the PVDF samples, had the lowest thermal conductivity. Perhaps, having higher are density can mean on having lower thermal conductivity than the ones with smaller area density, such as the

PVA samples and the copper foil.

Table 9. Area density analysis of the sample material

Material	Area density (g/cm^2)
PVA Pre-carbonized	0.00210
PVA Carbonized	0.00242
PVA Carbonized Copper Coated	0.00646
Copper Foil	0.09029
PVDF Pure	0.13862
PVDF Pt110 20wt%	0.12336
PVDF CCS100 20wt%	0.15659
PVDF NX10 20wt%	0.16300
PVDF Pt110 40wt%	0.19193
PVDF CCS100 40wt%	0.16037
PVDF NX10 40wt%	0.16110

Table 10. Thermal Conductivity of the samples measured using the thermal conductivity setup

Sample	Material	Measured k value(W/m*K)
1	PVDF NX10 20wt%	0.4194
2	PVDF Pt110 20wt%	0.4836
3	PVDF CCS100 20wt%	0.5311
4	PVDF NX10 40wt%	0.8249
5	PVDF Pt110 40wt%	0.8684
6	PVDF CCS100 40wt%	0.9630
7	PVA Pre-carbonized #1	7.8932
8	PVA Pre-carbonized #2	8.5813
9	PVA Carbonized #1	71.5891
10	PVA Carbonized #2	78.7029
11	PVA Carbonized #3	78.7029
12	PVA Carbonized #4	81.6179
13	PVA Carbonized Nitrogen Doped	78.2342
14	PVA Carbonized Silver Coated	92.9562
15	PVA Carbonized Copper Coated	159.0584

16	Copper Foil #1	363.2443
17	Copper Foil #2	363.2443

CHAPTER IV

CONCLUSIONS AND FUTURE WORK

A study was performed on the different types of nanomaterials, such as: carbon fibers, composites, mats, thin films, carbon nanotubes. In order to analyze what types of measurements they made, as well as their findings, which were going to be helpful when doing our own thermal conductivity measurements. Different thermal conductivity setups were studied as well, in order to see how they did measure the thermal conductivity, what type of method did they employ, and if the method used would be complicated. When evaluating thermal conductivity the best option is to evaluate the k value directly, not indirectly, meaning that the thermal conductivity should be solely evaluated and do not have any external factors influencing, such as: thermal diffusivity, specific heat, electrical resistivity, thermal resistivity, etc.

From this study, a custom made thermal conductivity setup was built, this setup is able to measure the thermal conductivity of nanomaterials, mainly based on nanofibers, and the setup measures in-plane thermal conductivity, but most importantly, it has a simple but effective path to calculate the thermal conductivity. When comparing the measured results from known materials against the thermal conductivity results found in literature, the results were not too far apart, showing this method to be an effective option to measure in-plane thermal conductivity. Also, when measuring unknown materials, both low and high thermal conductive materials were successfully measured. Pure PVDF, as well as samples of PVDF along with boron nitride served

as the low thermal conductivity materials. As for the high thermal conductivity materials, different types of PVA fibers were evaluated, going from pre-carbonized to carbonized with different fillers, in order to evaluate how would the thermal conductivity be affected. Comparing the pre-carbonized fibers with the carbonized fibers, showed an increment in the carbonized fibers of almost 10 times what was measured from the pre-carbonized sample. As for, the carbonized sample with fillers, the sample that was coated with copper, showed an enhancement on the thermal conductivity of 2 times what was measured for the carbonized sample.

In addition to the results presented above, the author would like to further expand this project. A through-plane thermal conductivity tester would be a great addition, thus having to custom made thermal conductivity setup, one that measured in-plane thermal conductivity, and another that measures thermal conductivity. Perhaps, modifications can be made to the setup presented in this work, in order to make it measure both in-plane and through-plane thermal conductivity.

REFERENCES

- [1] N.C. Gallego, D.D. Edie, B. Nysten, J.P. Issi, J.W. Treleven, G.V. Deshpande, (2000) The thermal conductivity of ribbon-shaped carbon fibers (1999) *Carbon* 38 1003–1010
- [2] WANG Jian-li, GU Ming, MA Wei-gang, ZHANG Xing, SONG Yan, Temperature dependence of the thermal conductivity of individual pitch-derived carbon fibers *NEW CARBON MATERIALS*, Volume 23, Issue 3, March 2008
- [3] Hyun-kyu Shin, Hong-Bum Lee, Kwang-Soo Kim, (2000) Tribological properties of pitch-based 2-D carbon-carbon composites *Carbon* 39 (2001) 959–970
- [4] William Marshall Moses, Jr, (1978) Measurement of Thermal Conductivity of PAN Based Carbon Fiber Georgia Institute of Technology, March, 1978
- [5] N.C Gallego, D.D Edie, Structure–property relationships for high thermal conductivity carbon fibers (2001) *Composites: Part A* 32 (2001) 979-980
- [6] CHEN Jie, LONG Ying, XIONG Xiang, XIAO Peng, (2012) Microstructure and thermal conductivity of carbon/carbon composites made with different kinds of carbon fibers *J. Cent. South Univ.* (2012) 19: 1780–1784
- [7] Seungjin Han, Jan T. Lin, Yasuhiro Yamada, D.D.L. Chung, (2008) Enhancing the thermal conductivity and compressive modulus of carbon fiber polymer–matrix composites in the through-thickness direction by nanostructuring the interlaminar interface with carbon black *CARBON* 46 (2008) 1060–1071
- [8] Korab J, Stefanik P, Kavecky S, Sebo P, Korb G, (2002) Thermal conductivity of unidirectional copper matrix carbon fibre composites *Composites: Part A* 33(2002) 577-581
- [9] Fukai Jun, Makoto Kanou, Kodama Yoshikazy, Miyatake Osamu, (2000) Thermal conductivity enhancement of energy storage media using carbon fibers *Energy Conversion & Management* 41 (2000) 1543-1556
- [10] Ordonez-Miranda Jose, Yang Ronggui, (2015) Effect of a metallic coating on the thermal

conductivity of carbon nanofiber-dielectric matrix composites *Composites Science and Technology* 109 (2015) 18–24

- [11] Zhang X, Fujiwara S, Fujii M, (1999) Measurements of Thermal Conductivity and Electrical Conductivity of a Single Carbon Fiber *International Journal of Thermophysics*, Vol. 21, No. 4, 2000
- [12] May P.W, Portman R, Rosser K.N, (2005) Thermal conductivity of CVD diamond fibres and diamond fibre-reinforced epoxy composites *Diamond & Related Materials* 14 (2005) 598– 60
- [13] Wolter S.D, Borca-Tasciuc D.A, Chen G, Govindaraju N, Collazo R, Okuzumi F, Prater J.T, Sitar Z (2003) Thermal conductivity of epitaxially textured diamond films *Diamond and Related Materials* 12 (2003) 61–64
- [14] Ma Zhaokun, Shi Jingli, Song Yang, Guo Quanguai, Zhai Gentai, Lang Liu, (2006) Carbon with high thermal conductivity, prepared from ribbon-shaped mesophase pitch-based fibers *Carbon* 44 (2006) 1298–1352
- [15] Mayhew Eric, Prakash Vikas, (2013) Thermal conductivity of individual carbon nanofibers *CARBON* 62 (2013) 493–500
- [16] R.D Patton, C.U. Pittman Jr, L. Wang, J.R. Hill, A. Day, (2001) Ablation, mechanical and thermal conductivity properties of vapor grown carbon fiber-phenolic matrix composites *Composites: Part A* 33(2002) 243-251
- [17] Ai-jie Ma, Hongchun Li, Weixing Chen, and Yonggang Hou, Improved (2013) Thermal Conductivity of Silicon Carbide/Carbon Fiber/Epoxy Resin Composites *Polymer-Plastics Technology and Engineering*, 52: 295–299, 2013
- [18] Hyun Su Kim , Ji-un Jang , Jaesang Yu , Seong Yun Kim, (2015) Thermal conductivity of polymer composites based on the length of multi-walled carbon nanotubes *Composites Part B* 79 (2015) 505e512
- [19] Ng Yen Hsiao, Lu Xuehong, Lau Khim Soo, (2005) Thermal Conductivity, Electrical Resistivity, Mechanical, and Rheological Properties of Thermoplastic Composites Filled With Boron Nitride and Carbon Fiber *POLYM. COMPOS.*, 26:66–73, 2005.
- [20] Valipour Peiman, Babaahmadi Vahid, Nasouri Komeil, (2014) Fabrication of Poly(methyl methacrylate) Nanofibers and Polyethylene Nonwoven with Sandwich Structures for Thermal Insulator Application *Advances in Polymer Technology*, Vol. 33, No. S1, 2014,
- [21] Khan W.S, Asmatulu R, Rodriguez V, Ceylan M, (2014) Enhancing thermal and ionic conductivities of electrospun PAN and PMMA nanofibers by graphene nanoflake

additions for battery-separator applications Int. J. Energy Res. 2014; 38:2044–2051

- [22] Kausar Ayesha, Ashraf Rozina, (2014) Electrospun, non-woven, nanofibrous membranes prepared from nano-diamond and multi-walled carbon nanotube-filled poly(azo-pyridine) and epoxy composites reinforced with these membranes Journal of Plastic Film & Sheeting 2014, Vol. 30(4) 369–387
- [23] Liang Junfeng, Saha Mrinal C, Altan Cengiz M, (2013) Effect of carbon nanofibers on thermal conductivity of carbon fiber reinforced composites Procedia Engineering 56 (2013) 814– 820
- [24] Weidenfeller Bern, Hofer Michael, Schilling Frank, (2004) Thermal conductivity, thermal diffusivity, and specific heat capacity of particle filled polypropylene Composites: Part A 35 (2004) 423–429
- [25] Kuriger Rex, Alam M. Khariul, (2002) Thermal conductivity of thermoplastic composites with submicrometer carbon fibers Experimental Heat Transfer, 15:19–30, 2002
- [26] Kim Ji-Hoo, Kim Gue-Hyun, (2014) Effect of Orientation and Content of Carbon Based Fillers on Thermal Conductivity of Ethylene-Propylene-Diene/Filler Composites Division of Energy and Bio Engineering, Dongseo University, Busan 617-716, South Korea
- [27] Xu Yusheng, Chung D.D.L, (2000) Cement of high specific heat and high thermal conductivity, obtained by using silane and silica fume as admixtures Cement and Concrete Research 30 (2000) 1175-1178
- [28] Khedari Joseph, Watsanasathaporn Pornnapa, Hirunlabh Jongit, (2005) Development of fibre-based soil-cement block with low thermal conductivity Cement & Concrete Composites 27 (2005) 111–116
- [29] Khedari Joseph, Suttisons Borisut, Pratinthong Naris, Hirunlabh Jongjit, (2001) New lightweight composite with low thermal conductivity Cement and Concrete Composites 23 (2001) 65-70
- [30] Zha Jun-Wei, Dang Zhi-Min, Li Wei-Kang, Zhu Yan-Hui, Chen George, (2014) Effect of Micro- Si₃N₄–nano-Al₂O₃ Co-filled Particles on Thermal Conductivity, Dielectric and Mechanical Properties of Silicone Rubber Composites IEEE Transactions on Dielectrics and Electrical Insulation Vol. 21, No. 4; August 2014
- [31] Satyala Nikhul, Rad Armin, Zamanipour Zahra, Norouzzadeh Payam, Krasinski Jerzy, Tayebi Lobat, Vashae Daryoosh, (2014) Reduction of thermal conductivity of bulk nanostructured bismuth telluride composites embedded with silicon nano-inclusions

- [32] Barucci M, Bianchini G, Del Rosso T, Gottardi E, Peroni I, Ventura G, (2000) Thermal expansion and thermal conductivity of glass-fibre reinforced nylon at low temperature *Cryogenics* 40 (2000) 465±467
- [33] Asako Yutaka, Kamikoga Hisajoshi, Nishimura Hisani, Yishiyuki Yamaguchi, (2002) Effective thermal conductivity of compressed woods *International Journal of Heat and Mass Transfer* 45 (2002) 2243–2253
- [34] Thunman Henrik, Leckner Bo, (2002) Thermal conductivity of wood—models for different stages of combustion *Biomass and Bioenergy* 23 (2002) 47 – 54
- [35] Barabash V, Mazul I, Latypov R, Pokrovsky A, Wu C.H, (2002) The effect of low temperature neutron irradiation and annealing on the thermal conductivity of advanced carbon-based materials *Journal of Nuclear Materials* 307–311 (2002) 1300–1304
- [36] Snead L.L, Balden M, Causey R.A, Atsumi H, (2002) High thermal conductivity of graphite fiber silicon carbide composites for fusion reactor application *Journal of Nuclear Materials* 307–311 (2002) 1200–1204
- [37] Kalaprasad G, Pradeep P, Mathew George, Pavithran C, Thomas Sabu, (2000) Thermal conductivity and thermal diffusivity analyses of low-density polyethylene composites reinforced with sisal, glass and intimately mixed sisal/glass fibres *Composites Science and Technology* 60 (2000) 2967±2977
- [38] Tavman I.H, Akinea H, (2000) Transverse thermal conductivity of fiber reinforced polymer composites *Int. Corant Heat Mass Transfer*, Vol. 27, No. 2, pp. 253-261, 2000
- [39] Gobbe Claire, Iserna Sebastien, Ladevie Bruno, (2004) Hot strip method: application to thermal characterization of orthotropic media *International Journal of Thermal Sciences* 43 (2004) 951–958
- [40] Ren Liyun, Pashayi Kamyar, Fard Hafez, Kotha Shiva, Borca-Tasciuc Theodorian, Ozisik Rahmi, (2013) Engineering the coefficient of thermal expansion and thermal conductivity of polymers filled with high aspect ratio silica nanofibers *Composites: Part B* 58 (2014) 228–234
- [41] Berbon Min, Dietrich Donald, Marshall David, (2001) Transverse thermal conductivity of thin C/SiC composites fabricated by slurry infiltration and pyrolysis *Journal of the American*

- [42] Agrawal Richa, Saxena N.S, Sreekala M.S, Thomas S, (1999) Effect of Treatment on the Thermal Conductivity and Thermal Diffusivity of Oil-Palm-Fiber-Reinforced Phenolformaldehyde Composites Condensed Matter Physics Lab, Department of Physics, University of Rajasthan, Jaipur
- [43] Gumen V, Haq A., Myaa B, Maqsood A, High-Temperature Thermal Conductivity of Ceramic Fibers (2001) JMEPEG (2001) 10:475–478
- [44] Kanagaraj S, Pattanayak S, (2004) Low temperature thermal conductivity of woven fabric glass fibre composites Cryogenic Engineering Centre, Indian Institute of Technology, Kharagpur, West Bengal, 721 302, India
- [45] Bailleul J, Deleunay D, Jarny Y, Jurkowski T, (2001) Thermal Conductivity of Unidirectional Reinforced Composite Materials—Experimental Measurement as a Function of State of Cure Laboratoire de Thermocinétique (UMR CNRS 6607)
- [46] Lee Sang Heon, Choi Yong, (2014) Effect of Nano-Sized Oxide Particles on Thermal and Electrical Properties of Epoxy Silica Composites The Physics of Metals and Metallography, 2014, Vol. 115, No. 13, pp. 1295–1299
- [47] Gao Zhifang, Zhao Lei, (2015) Effect of nano-fillers on the thermal conductivity of epoxy composites with micro-Al₂O₃ particles Materials and Design 66 (2015) 176–182
- [48] Donnay Martin, Tzcalas Spiros, Logakis Emmanuel, (2015) Boron nitride filled epoxy with improved thermal conductivity and dielectric breakdown strength Composites Science and Technology 110 (2015) 152–158
- [49] Fu Shao-Yun, Mai Yiu-Wing, (2002) Thermal Conductivity of Misaligned Short-Fiber-Reinforced Polymer Composites Technical Institute of Physics and Chemistry, Chinese Academy of Sciences, Beijing 100080, China
- [50] Li Zhiliang, Zheng Shuqi, Huang Ting, Zhang Yuzhuo, Teng Renyuan, Lu Guiwu, Rational design, high-yield synthesis, and low thermal conductivity of Te/Bi₂Te₃ core/shell heterostructure nanotube composites (2014) Journal of Alloys and Compounds 617 (2014) 247–252
- [51] Stacy Shawn, Zhang Xin, Pantoya Michelle, Weeks Brandon, The effects of density on thermal conductivity and absorption coefficient for consolidated aluminum nanoparticles (2014) International Journal of Heat and Mass Transfer 73 (2014) 595–599
- [52] Lee Sang Hyun, kwon Su Yong, Ham Hye Jeong, Thermal conductivity of tungsten–copper composites (2012) Thermochimica Acta 542 (2012) 2– 5

- [53] Shen Xiao-Yu, He Xin-Bo, Ren Shu-Bin, Zhang Hao-Ming, Que Xuan-Hui, Effect of molybdenum as interfacial element on the thermal conductivity of diamond/Cu composites (2012) *Journal of Alloys and Compounds* 529 (2012) 134–139
- [54] Harish Sivasankaran, Orejon Daniel, Takata Yasuyuki, Kohno Masamichi, Thermal conductivity enhancement of lauric acid phase change nanocomposite with graphene nanoplatelets (2015) *Applied Thermal Engineering* 80 (2015) 205–211
- [55] Fang Lijun, Wu Chao, Qian Liyuan, Yang Ke, Jiang Pingkai, Nano–micro structure of functionalized boron nitride and aluminum oxide for epoxy composites with enhanced thermal conductivity and breakdown strength (2014) *RSC Adv.*, 2014, 4, 21010
- [56] Foley Brian, Brown-Shaklee Harlan, Duda John, Cheaito Ramez, Gibbons Brady, Medlin Doug, Ihlefeld Jon, Hopkins Patrick, Thermal conductivity of nano-grained SrTiO₃ thin films (2012) *APPLIED PHYSICS LETTERS* 101, 231908 (2012)
- [57] Carlos Silva, Egidio Marotta, Michael Schuller, In-plane thermal conductivity in thin carbon fiber composites (2007) *Journal of thermophysics and heat transfer* vol.21, No. 3, July- September 2007
- [58] Bing Wang, Yingde Wang, Effect of Fiber Diameter on Thermal Conductivity of the Electrospun Carbon Nanofiber Mats (2011) *Advanced Materials Research* Vols. 332-334 (2011) pp 672-677
- [59] Nayandeep K. Mahanta, Alexis R. Abramson, Max L. Lake, David J. Burton, John C. Chang, Helen K. Mayer, Jessica L. Ravine, Thermal conductivity of carbon nanofiber mats (2010) *CARBON* 48 (2010) 4457–4465
- [60] Han Yan, Nayandeep K. Mahanta, Laurent J. Majerus, Alexis R. Abramson, Miko Cakmak, Thermal Conductivities of Electrospun Polyimide-Mesophase Pitch Nanofibers and Mats (2014) *POLYM. ENG. SCI.*, 54:977–983, 2014.
- [61] Park Joung-Man, Kwon Dong-Jun, Wang Zuo-Jia, Roh Jeong-U, Lee Woo-Il, Park Jong-Kyoo, DeVries K. Lawrence, Effects of carbon nanotubes and carbon fiber reinforcements on thermal conductivity and ablation properties of carbon/phenolic composites (2014) *Composites: Part B* 67 (2014) 22–29
- [62] Xing Yajuan, Cao Wei, LI Wei, Chen Jongyuan, Wang, Miao, Wei Hanxing, Hu Dongmei, Chen Minghai, Li Qingwen, Carbon Nanotube/Cu Nanowires/Epoxy Composite Mats with Improved Thermal and Electrical Conductivity (2015) *Journal of Nanoscience and Nanotechnology* Vol. 15, 3265–3270, 2015
- [63] Price Duncan, Jarratt Mark, Thermal conductivity of PTFE and PTFE composites (2002) *Thermochimica Acta* 392–393 (2002) 231–236

- [64] Andrew J. Bullen, Keith E. O'Hara, and David G. Cahill, Thermal conductivity of amorphous carbon thin films (2008) Department of Materials Science and Engineering, Coordinated Science Laboratory, and Materials Research Laboratory, University of Illinois, Urbana, Illinois 61801
- [65] Sweeting R.d, Lui X.L, Measurement of thermal conductivity for fibre-reinforced composites (2004) Composites: Part A 35 (2004) 933–938
- [66] Kandare Everson, Khatibi Akbar, Yoo Sanghyun, Wang Ruoyu, Ma Jun, Olivier Philippe, Gleizes Nathalie, Wang Chun, Improving the through-thickness thermal and electrical conductivity of carbon fibre/epoxy laminates by exploiting synergy between graphene and silver nano-inclusions (2015) Composites Part A Applied Science and Manufacturing · November 2014
- [67] Kato R, Maesono A, Tye R.P, Thermal Conductivity Measurement of Submicron-Thick Films Deposited on Substrates by Modified ac Calorimetry (Laser-Heating Angstrom Method) (2001) International Journal of Thermophysics, Vol. 22, No. 2, 2001
- [68] Zheng D, Tanaka S, Miyazaki K, Takashiri M, Evaluation of Specific Heat, Sound Velocity and Lattice Thermal Conductivity of Strained Nanocrystalline Bismuth Antimony Telluride Thin Films (2015) Journal of ELECTRONIC MATERIALS, Vol. 44, No. 6, 2015
- [69] Yan Wei, Sun Huawei, Liu Siwei, Chi Zhenguo, Chen Xudong, Xu Jiarui, Polyimide nanocomposites with boron nitride-coated multi-walled carbon nanotubes for enhanced thermal conductivity and electrical insulation (2014) J. Mater. Chem. A, 2014, 2, 20958
- [70] Donovan Brian, Foley Brian, Ihlefeld Jon, Maria Jon-Paul, Hopkins Patrick, Spectral phonon scattering effects on the thermal conductivity of nano-grained barium titanate (2014) APPLIED PHYSICS LETTERS 105, 082907 (2014)
- [71] Tang G.H, Bi C, Fu B, Thermal conduction in nano-porous silicon thin film (2013) JOURNAL OF APPLIED PHYSICS 114, 184302 (2013)
- [72] Motoo Fujii, Xing Zhang, Huaqing Xie, Hiroki Ago, Koji Takahashi, Tatsuya Ikuta, Hidekazu Abe, Tetsuo Shimizu, Measuring the Thermal Conductivity of a Single Carbon Nanotube (2005) PRL 95, 065502 (2005)
- [73] Mohamed A Osman, and Deepak Srivastava, Temperature dependence of the thermal conductivity of single-wall carbon nanotubes (2001) NASA Ames Research Center, Moffett Field, CA 94035 and School of Electrical Engineering and Computer Science, Washington State University, Pullman, WA 99164-2752, USA
- [74] Young Jin Heo, Chang Hun Yun, Woo Nyon Kim, Heon Sang Lee, The effect of mesoscopic

- shape on thermal properties of multi-walled carbon nanotube mats (2011) *Current Applied Physics* 11 (2011) 1144e1148
- [75] Tang Guodong, Yang Wenchao, Wen Jianfeng, Wu Zhuangchun, Fan Can, Wang Zhihe, Ultra low thermal conductivity and thermoelectric properties of carbon nanotubes doped (2015) *Ceramics International* 41 (2015)961–965
- [76] Li Shi, Deyu Li, Choongho Yu, Wanyoung Jand Dohyung Kim, Zhen Yao, Philip Kim, Arunava Majumdar Measuring Thermal and Thermoelectric Properties of One-Dimensional Nanostructures Using a Microfabricated Device (2003)
- [77] Arden L Moore, Li Shi, On errors in thermal conductivity measurements of suspended and supported nanowires using micro-thermometer devices from low to high temperatures (2010)
- [78] Kalnin, I. L., "Thermal Conductivity of High-Modulus Carbon Fibers", Composite Reliability, ASTM STP 580, American Society for Testing and Materials, p. 560.
- [79] Schroder, J., "Apparatus for Determining the Thermal Conductivity of Solids in the Temperature Range from 20 to 200C", TheReviewofScientificInstruments, 34, p. 615.
- [80] F. Frusteri, V. Leonardi, S. Vasta, G. Restuccia, Thermal conductivity measurement of a PCM based storage system containing carbon fibers (2004)
- [81] Balandin A, Ghosh S, Bao W, Calizo I, Teweldebrhan D, Miao F, Lau C. N, Extremely High Thermal Conductivity of Graphene: Experimental Study (2007-2008)
- [82] Nayandeep K. Mahanta, Alexis R. Abramson, The dual-mode heat flow meter technique: A versatile method for characterizing thermal conductivity (2010)

APPENDIX

APPENDIX

NOMENCLATURE

Symbol	Description	Units
A	Cross-sectional area	m^2
d	Distance between thermocouples T1 and T2	m
k	Thermal Conductivity	$\frac{W}{m \cdot K}$
ΔT	Difference in temperature	K
q	Heat flow	$\frac{W}{m^2}$
D	Density	$\frac{kg}{m^3}$
C_p	Specific Heat	$\frac{J}{K \cdot m^3}$
α	Thermal Diffusivity	$\frac{m^2}{s}$
G	Thermal Conductance	$\frac{W}{K}$
L	Length	m
Q	Heat	W
T	Temperature	K
Δe	Potential drop	Ω
ρ_e	Electrical resistivity	$\Omega \cdot cm$
t	Time	s
V	Voltage	V
I	Current	A
P	Perimeter	m

BIOGRAPHICAL SKETCH

Javier Acosta Martinez received his Bachelors of Science from the University of Texas – Pan American (UTPA) in May 2014. While an undergraduate, he was involved in many student organizations such as Society of Hispanic Professional Engineers (SHPE), American Society of Mechanical Engineers (ASME). In his senior semester, Javier, took a position as an undergraduate research assistant in Dr. Lozano’s PREM team, where his research focused on the development of PVA nanofibers utilizing the Forcespinning™ method. As a graduate student Javier focused on measuring the thermal conductivity of nanomaterials, by creating a custom made setup. Javier received his Master of Science in Mechanical Engineering from The University of Texas Rio Grande Valley (UTRGV) in May 2016. For correspondence, email javy_acosta@hotmail.com.